

AN INVESTIGATION OF FOCUSED ION BEAM MICROMACHINING

THESIS

Presented to the Graduate Council
of Texas State University–San Marcos
in Partial Fulfillment
of the Requirements

for the Degree

Master of SCIENCE

By

Nelson W. White, B.S.

San Marcos, Texas
May, 2005

COPYRIGHT

by

Nelson W. White

2005

DEDICATION

I would like to dedicate this thesis to my father, Nelson White, for instilling a curiosity for science and learning; to Mammam (Melba Moore, my grandmother) for encouraging me and convincing me to believe in myself and for always believing in me even when I did not; my sister, Page Warren, for being my friend and supporting me in all of my endeavors; and most especially to my mother, Gail McClellan, who always believed in me and made it all possible.

ACKNOWLEDGEMENTS

I would like to begin by thanking the members of my family for the support and patience throughout the process of accomplishing this goal. Specifically I would like to thank my sister, Page, for supporting me and being my personal cheerleader and my mother, Gail, for always giving me the courage and strength I needed to complete my goals.

I am very thankful to the members of my thesis committee, Dr. Carlos J. Gutierrez, Dr. Ir. Wilhemus J. Geerts and Dr. Victor E. Michalk for their patience and direction in this endeavor. I would like add a special thanks to Dr. Carlos J. Gutierrez, for his support and direction throughout this effort. I will always be grateful for the extra effort he put into helping me accomplish this goal by going the extra mile and who without his continued support this would not have been possible.

Thanks to Philips Semiconductors for allowing me the time, as well as providing the equipment, to pursue this work. Special thanks to Annette Garcia for her time and patience. She was instrumental in training me in the techniques and use of the equipment.

I would like to thank Paul Person, Charlie Watts, Michael Matheaus, Kevin Wiederhold, Eric Wittry, Yuji Yamaguchi, and Matt Langendorf for being my “compadres,” each in turn helping me to

understand the more difficult material and keeping me up to speed as I struggled balancing full time student and full time employee. You guys were the best of friends and I'll never forget you. I would also like to thank Norma Cardona for supporting me in this endeavor.

This manuscript was submitted on January 12, 2005.

TABLE OF CONTENTS

ACKNOWLEDGEMENTS.....	v
LIST OF TABLES	ix
LIST OF FIGURES	x
1 INTRODUCTION.....	1
1.1 IMPORTANCE OF THE FOCUSED ION BEAM IN THE MICROELECTRONICS INDUSTRY	1
1.2 OVERVIEW OF EXPERIMENTS, WORK AND PHYSICAL CHARACTERIZATION METHODS USED	4
1.3 THESIS PROJECT GOALS.....	5
2 FOCUSED ION BEAM THEORY, TECHNIQUES AND APPLICATIONS	7
2.1 THE FIB	7
2.1.1 THE ION BEAM	7
2.1.2 THE COLUMN	12
2.1.3 ION – MATTER INTERACTION	18
2.2 FOCUSED ION BEAM APPLICATIONS	23
2.2.1 INTEGRATED CIRCUIT FAILURE ANALYSIS	24
2.2.2 CROSS SECTIONING.....	25
2.2.3 TEM SAMPLE PREPARATION	29
2.2.4 MICROMACHINING.....	30
2.3 DUAL BEAM SYSTEMS	30
3 SAMPLE DATA AND ANALYSIS	33
3.1 OVERVIEW OF SETUP	33
3.1.1 THE TOOL.....	33
3.1.2 FOCUSING AND BEAM SETUP.....	34
3.1.3 THE EUCENTRIC POINT.....	39
3.2 SAMPLE 1 - FAILURE ANALYSIS OF AN INTEGRATED CIRCUIT	42
3.3 SAMPLE 2 - MATERIAL DEPOSITION.....	46
3.4 SAMPLES 3-5 - MICROMACHINING	49
3.4.1 LEARNING.....	50
3.4.2 SAMPLE 3	56

3.4.3	COMPLEX SHAPES	60
4	CONCLUSION	65
	BIBLIOGRAPHY.....	68

LIST OF TABLES

Table 2-1 Precision and uses of various cross sectioning techniques.....	25
Table 3-1 Recommended Beam Currents.	38
Table 3-2 SEM AVA Aperture Recommendations.	39

LIST OF FIGURES

Figure 2-1 Ion extraction in an electric field.	8
Figure 2-2 Gallium LMIS.	10
Figure 2-3 Schematic representation of a Taylor Cone with a 49° interior angle.	11
Figure 2-4 Current required to reach 750°C by emitter operating time ..	12
Figure 2-5 Half angle of the beam	14
Figure 2-6 Beam Deflection.	17
Figure 2-7 Simple image of beam with beam blanker and deflector.	18
Figure 2-8 Ion-Matter Interactions.....	19
Figure 2-9 Emission of Secondary Electrons for Imaging.....	19
Figure 2-10 Ion Beam Milling.	20
Figure 2-11 Gas enhanced etching.	22
Figure 2-12 Ion Enhanced Deposition.	23
Figure 2-13 Coarse Mill Scan Pattern.	26
Figure 2-14 Coarse Mill Cross Section.	26
Figure 2-15 The fine mill pattern is a much smaller than the coarse mill pattern.	28
Figure 2-16 The fine mill cleans-up the face of the cross section at the area of interest.	28

Figure 2-17 Comparison of various imaging techniques.	29
Figure 2-18 TEM sample preparation.	30
Figure 2-19 Dual Beam System.	31
Figure 3-1 FEI's Magnum Column.	33
Figure 3-2 Eucentric Height Described.	40
Figure 3-3 Scribeline test structure schematics.	43
Figure 3-4 Site of Failure: Post Coarse Milling.	44
Figure 3-5 M2-M2 Continuity Failure.	45
Figure 3-6 Platinum deposition.	47
Figure 3-7 Coarse Mill.	48
Figure 3-8 Fine Mill.	48
Figure 3-9 Example of Micromachining Layout.	49
Figure 3-10 Example of Excessive Ion Beam Exposure.	50
Figure 3-11 Example of parallel milling followed by a serial mill for cleanup.	51
Figure 3-12 Final result of micromachining wires using the parallel method.	52
Figure 3-13 Milling wires with a higher beam current followed by a cleaning mill.	53
Figure 3-14 Use of serial mode for milling provides much cleaner lines without redeposition.	54
Figure 3-15 Serial mode milling for wire isolation proved to have similar redeposition problems.	55

Figure 3-16 Serial mode with all regions being milled at the same time. 56

Figure 3-17 Mill pattern for first sample.57

Figure 3-18 Initial parallel mill of six section to create the wires.58

Figure 3-19 Isolation of the wires from the rest of the substrate.59

Figure 3-20 Attempts to remove the redeposited material ruined the
mached wires.59

Figure 3-21 Ion beam image of micromachined circle.60

Figure 3-22 SEM image of same circle at 52° tilt.60

Figure 3-23 Mill pattern for cylinders.61

Figure 3-24 Micromachined cylinders.61

Figure 3-25 Mill pattern for milling hexagons.61

Figure 3-26 Micromachining hexagons turned out to be the most difficult
shape to machine.62

Figure 3-27 Mill pattern for serpentine structures.63

Figure 3-28 SEM image of micromachined serpentine.63

Figure 3-29 Micro wires twice as long as previously.63

Figure 3-30 Grating pattern.....64

Figure 3-31 Milled grating.64

CHAPTER 1

INTRODUCTION

1.1 THE IMPORTANCE OF THE FOCUSED ION BEAM IN THE MICROELECTRONICS INDUSTRY

In today's world of computers and electronic devices the demand for high yield in the production of integrated circuits is essential to keep profitability at a maximum. To make this a reality it is necessary to understand the characteristic of failures if they are to be eliminated from the model from which all other microchips are made.

The microscope in general has always been the primary tool for defect investigation. As the technology of integrated circuits has advanced, and geometries have gotten smaller, the microscope has also advanced. The industry has moved from the standard optical microscope to SEM's to FIB's and more recently transmission electron microscopes (TEM's). Lower magnification microscopes, with greater depth of field and a wider field of view, are still widely used, however, as sub-micron IC's advance it is necessary to use higher resolution microscopes to image the devices. This drives the use of higher resolution microscopes such as SEM and FIB.²

Failure and yield analysis are performed to identify the root failure mechanism of a product so that the corrective action can be fed back to the manufacturing line to avoid future yield loss. There are many factors that play into successful failure analysis. Factors and disciplines that include: semiconductor physics, die technology processing, package technology, electrical engineering, basic metallurgy, basic chemistry and intuition. Failure analysis is typically performed on packaged products but can also be performed “in line” using wafer level techniques. These can consist of methodologies ranging from simple visual inspection to scanning electron microscopy (SEM) to electrical testing. As the critical dimensions of the integrated circuits get smaller and smaller it becomes increasingly more difficult to detect the root cause. One of the more recent tools being used is the focused ion beam (FIB) system.

In addition to being an advanced method of failure analysis the versatility of a FIB or FIB-SEM system makes it an excellent candidate for prototype work and micromachining.² The FIB can be used to machine any shape or structure in any type of substrate. In addition to being able to mill, or sputter, material it is also possible to deposit materials. With the right gases it is possible to deposit anything from insulators to conductors.⁸ Within the same tool it is possible to mill a via and fill it with a material making IC prototyping simpler and cheaper. The FIB can also take advantage of these capabilities to rewire existing integrated circuits to evaluate a design change.²

Focused ion beam systems have been in production for some time but have only been used in the microelectronics industry in the last ten years.⁸ FIB systems operate in a similar fashion to a SEM except rather than a beam of electrons FIB systems use a finely focused beam of gallium ions that can be operated at low beam currents for imaging or high beam currents for site specific milling or sputtering.⁸ At higher beam currents the FIB microscope can be used as an atomic scale milling machine to perform stress-free precision sectioning with sub-micron positional accuracy.³ This precision milling can also be used for precision micromachining on a scale from tens of millimeters to tens of nanometers. At lower beam currents FIB imaging resolution begins to rival SEM's in terms of imaging topography.⁸ The use of secondary electrons and secondary ions, the FIB's two imaging modes, produced by the ion beam offer many advantages over SEM.² The secondary electron images show intense grain orientation contrast.⁸ As a result grain morphology can be readily imaged without resorting to chemical etching. Grain boundary contrast can also be enhanced through careful selection of imaging parameters. The secondary ion images reveal chemical differences and are especially useful in corrosion studies.¹¹ Secondary ion yields of metals can increase by three orders of magnitude in the presence of oxygen revealing the presence of corrosion.⁸ Sectioning and imaging can be used to examine fragile and or challenging materials that would otherwise be extremely difficult to investigate. It is even possible

to prepare site-specific TEM samples with one-to-one correlation between TEM image and FIB image.⁸

These tools provide an effective arsenal in combating defects, characterizing failures and making device modifications. Several of these applications were explored in this thesis on a FEI Dual Beam workstation.

1.2 OVERVIEW OF EXPERIMENTS, WORK AND PHYSICAL CHARACTERIZATION METHODS USED

Several micromachining techniques and applications were reviewed and evaluated during this investigation of Focused Ion Beams. Multiple samples were provided by Dr. Gutierrez, Dr Geerts and Philips Semiconductors for the evaluation of several techniques. For all samples the FEI xP Dual Beam FIB with a gallium source was used.

The first sample was an integrated circuit chip that failed electrical testing for metal 2 to metal 2 continuity. This sample was provided by Philips Semiconductors. The objective was to use the FIB to find the failure and characterize it. Using the dual beam FIB it was possible to mill down to the failure. Once the correct location on the die was found, by the use of electrical CAD drawings, it was possible to find the failure. Through the use of a course mill and a serial cleanup mill it was determined that the metal 2 lines had failed to form properly thereby determining the root cause.

The next sample was also an integrated circuit provided by Philips Semiconductors. The objective for this test was to evaluate the benefits of material deposition. A platinum hard mask was deposited using a gas injection system and using the focused ion beam to disassociate the Pt depositing it on the wafer. After depositing the Pt it was used to protect the surface while milling down to look at the integrity of the underlying device.

Following work on integrated circuits, the focus moved to blanket substrates to evaluate the possibilities of micromachining structures on the samples. Several NiFe film samples were provided by Dr. Carlos Gutierrez and Dr. Anup Bandyapadhyay. Dr. Geerts also provided several samples for machining. On each of these samples a series of wires, cylinders and serpentine wires were machined into the material down to the substrate. Through trial and error it was discovered that the most effective way for getting clean cuts for all zones of machined area was to mill multiple zones in parallel with a series cleaning mill at low beam currents.

1.3 THESIS PROJECT GOALS

The semiconductor industry is quickly realizing the benefits of the FIB system and more recently the dual column FIB-SEM system for performing a wide range of applications on full wafer samples. This thesis investigates the physics of focused ion beam systems as well as dual beam systems. Investigations will occur in the areas of

micromachining and micro fabrication in the sub-micrometer regime. A study and review of the potential and benefits of a dual column system's capability when used for defect characterization, milling various materials and TEM sample preparation. Five case studies will be discussed including FIB techniques, failure analysis of an IC, micromachining various materials, micromachining various structures and material deposition. Experimental samples were supplied by Philips Semiconductors at San Antonio Texas, Dr. Carlos Gutierrez and Dr. Wilhemus Geerts of the Southwest Texas Physics department.

The experiments were conducted using a FEI xP Dual Beam workstation courtesy of Philips Semiconductors in San Antonio. The FIB was equipped with a gallium liquid metal ion source with a FEI Magnum column.

CHAPTER 2

FOCUSED ION BEAM THEORY, TECHNIQUES AND APPLICATIONS

2.1 THE FIB

The FIB system is, simply put, an ion beam that is generated from an ion source then focused through a chamber of optics onto a sample while operating in a vacuum. The three main components of the system are the source, the ion column and the beam writing mechanism. This can be used for imaging, milling, deposition and implantation on a sample.

2.1.1 THE ION BEAM

The two primary ion emission sources are gas field ionization sources and liquid metal ion sources. Ion formation from liquid metal ion sources (LMIS) were first studied by Krohn in the early 1960's and later in the early 1970's another group demonstrated a focused ion beam using a gas field ionization source (GFIS). General use FIB and SEM-FIB systems make use of the LMIS although some work has been done to try and improve GFIS performance due to some advantages of the very small source size.¹¹ Primary focus will be given to the LMIS and more specifically to gallium.

Liquid metal ion sources are from a class known as electrohydrodynamic (EHD) sources and were first used in FIB systems in 1978.¹¹ The beam from a gallium LMIS has been shown to have a brightness of 0.9×10^5 A/cm²steradian at 21 kV and an energy spread of 12eV at 10 μ A total current. Several other materials are available, such as gold, cesium and mercury, however all have much lower outputs or are not cost effective. Recently some alloys have been experimented with but have not progressed to a point of maturity.¹¹

For a LMIS to emit ions two things must occur. First, a cone must be developed in an electric field with a small enough tip radius that field evaporation can occur when exposed to an electric field. Once the cone, or tip, is formed the production of ions occurs by field evaporation.⁴

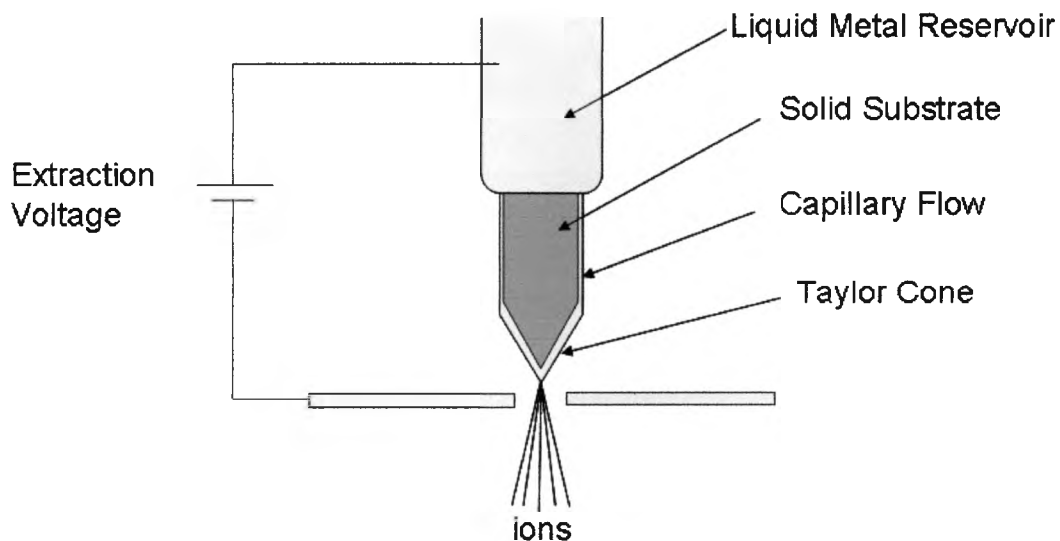


Figure 2-1: Ion extraction in an electric field.⁴

The electric field on an emitter is generated by applying a high voltage (Figure 2-1) to the emitter which is made of a single crystal refractory metal such as W or Rh. The field E at the emitter apex is proportional to $1/r$, where r is the end radius of the apex. Gas molecules are attracted to the region of high electric field at the emitter apex by the change in their polarization energy $\frac{1}{2} \alpha E^2$ where α is polarizability.¹¹

Today's focused ion beam systems have ion beams with a focus spot size of less than $1\mu\text{m}$ with a current density in the focused spot of $J=1\text{A}/\text{cm}^2$.¹¹ The majority of these beams being used in mainstream today are generated from a liquid metal ion source (LMIS) which is most often made of gallium. The LMIS uses the quantum mechanical field emission/field evaporation mechanism, appearing at high electric field strengths, for ionization of metal ions such as Ga, In or Au-Si-alloys. The molten metal covers a sharp emitter needle, generally made of tungsten, which takes a voltage of +8kV, with respect to an extraction electrode aperture. Therefore, the high field strength at the emitter tip enables the metal atoms to evaporate and ionize. They are extracted through the extraction aperture and can be further accelerated through the column.¹¹

The gallium LMIS provides very high brightness and high angular intensity. The intensity is about $17\mu\text{A}/\text{steradian}$ (1 sphere = 4π steradians) and the brightness is about $10^6 \text{ A}/\text{cm}^2/\text{steradian}$. A potential barrier holds atomic electrons near the nucleus. Applying very high electric field (about $10^8 \text{ V}/\text{cm}$) to field emission ion sources deforms

the potential barrier. This results in an appreciable probability that one or more electrons will tunnel through the barrier leaving behind a positively charged ion.¹² Figure 2-2 is an example of a gallium LMIS used by FEI.

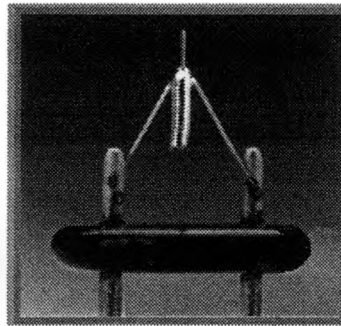


Figure 2-2: Gallium LMIS¹²

A strong electric field applied to the LMIS produces a tip with a very small radius. The source consists of a metal substrate, the emitter, is shaped in a conical form with a 49° half angle at the end. This half angle roughly approximates the shape of the liquid metal cone that the applied electric field will create on the surface of the substrate. This substrate is coated by the Ga.¹¹

Placing a high negative voltage on the extraction electrode applies the electric field to the LMIS. A strong enough electric field stresses the gallium covering the substrate into a “Taylor Cone”. (Figure 2-3) The Taylor cone is a conical extension produced at the end of the LMIS by

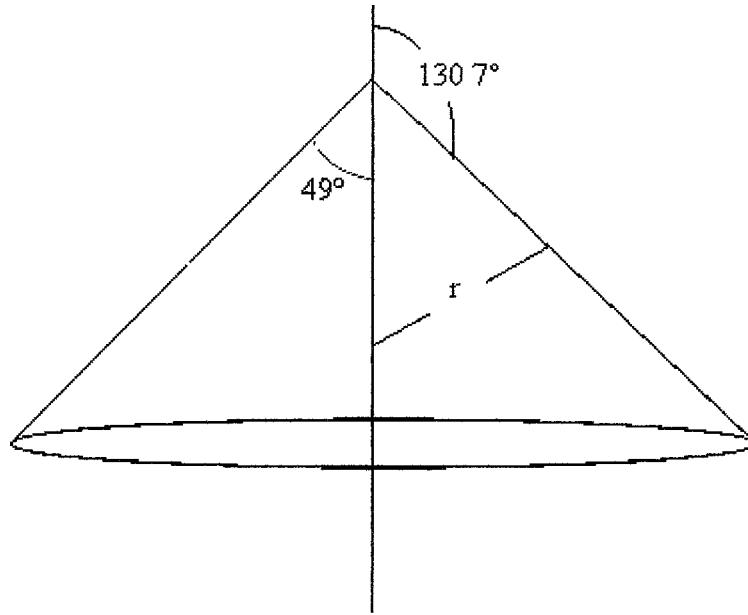


Figure 2-3: Schematic representation of a Taylor Cone with a 49° interior angle.¹¹

applying voltage to the metal substrate. The field and the counterbalancing surface tension in the liquid determine the half angle of the cone. This deformation will only occur after applying an electric field of sufficient strengths. Once the critical voltage is reached the cone forms and emission will begin. Once the emission process starts, the current rises approximately 200 μ A/kV of applied voltage. At this point the current density at the surface of the liquid reaches approximately 10⁸A/cm². At the leading edge of the LMIS Taylor cone, a protrusion with an end radius of approximately 20 \AA will appear. Ion emission due to field evaporation occurs at this protrusion.¹² The performance of a source is measured by its brightness and is defined as:

$$B = \left(\frac{I_s}{A_s \Omega_s} \right),$$

with units $A/cm^2steradian$.³ I_s is the current emitted by an area A_s of the source into an angle Ω_s . The solid angle into which a source emits ions is changed if a voltage, V_s , exists between the source and the point of measurement. The specific brightness $\beta=B/V_s$ is a more appropriate parameter however the brightness B is most often quoted.³

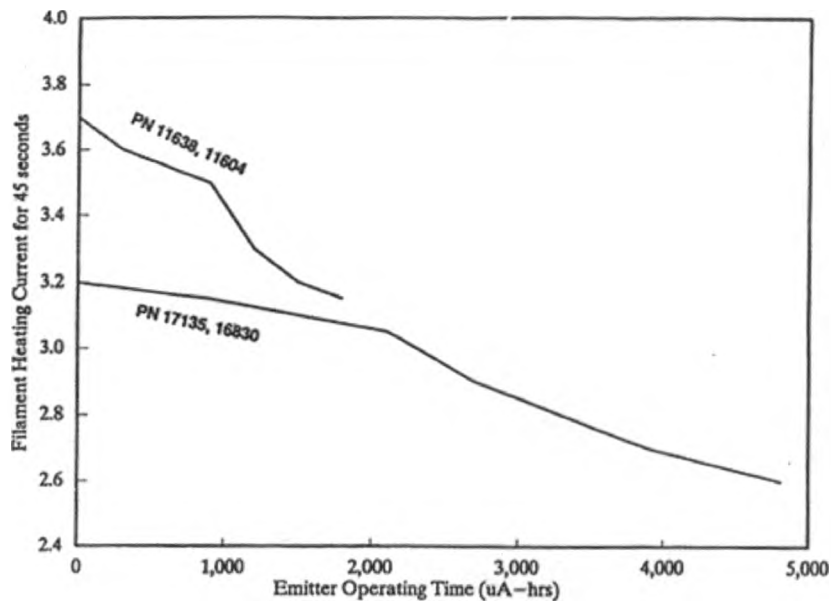


Figure 2-4: Current required to reach $750^{\circ}C$ by emitter operating time.¹²

2.1.2 THE COLUMN

The next main component of the FIB system is the column which focuses ions from the source onto the sample is very much like a series of optical lenses which may focus a source of light in one plane onto another plane.³ The column houses the LMIS, one or two electrostatic lenses (the optics), a set of blanking plates, beam acceptance aperture (BAA), an automatically variable aperture (AVA), and a deflector

(generally parallel plates or an octopole). Inside the column a structure secures and aligns the focusing elements. The LIMIS mounts on a stage that aligns the source with the center axis of the column. The ion column operates in a high vacuum environment to avoid interference from atmospheric gas molecules. This is achieved by using a metal chamber and an ion pump and a vacuum pump.¹²

The ion column mainly contains the electrostatic ion lenses but may also contain mass separators if alloy sources are used. These focus the ions from the LMIS onto the sample surface. In most operating regimes, the beam spot size and current density are limited by chromatic aberration and the virtual source size. Therefore the total beam diameter focused on a sample is given by:

$$d = (d_0^2 M^2 + d_c^2)^{1/2}$$

where d_0 is the virtual source size, M is the magnification and d_c is the contribution due to chromatic aberration.^{4, 7}

$$d_c = 2C_{co} M \alpha_0 \frac{\Delta E}{E}$$

C_{co} is the chromatic aberration coefficient referred to the source side and α_0 is the half angle of the beam accepted by the beam defining aperture (Figure 2-5), M is the magnification of the system, E is the final energy of the ions and ΔE is the energy spread.^{4,7} While the beam diameter expression is rather simple the chromatic aberration coefficient C_{co} is much more complicated when considered with its dependence on the

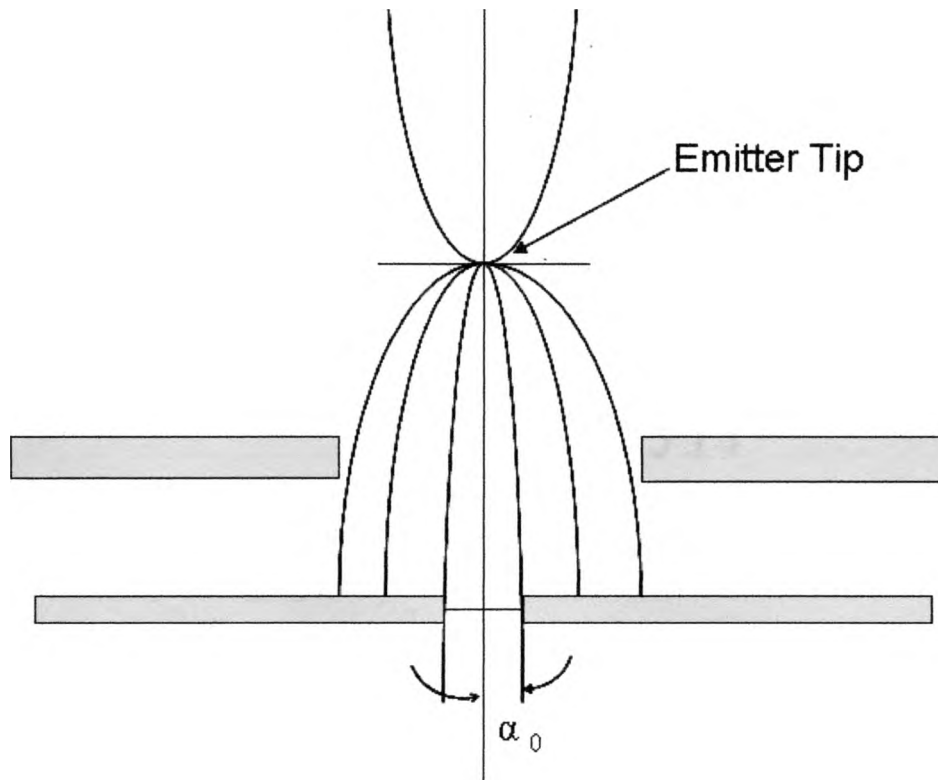


Figure 2-5: Half angle of the beam.⁴

layout of the electrodes and the value of the electrode potentials in all of the electrostatic lenses in an ion column. Ray tracing computer programs are used to calculate the aberration coefficients.⁴ It is also possible to do a reverse calculation to determine what constraints will minimize the aberration coefficient. A low aberration lens system designed in a more conventional fashion can predict a current density up to 20 times higher than previously reported.⁴ This is achieved in part by reducing the working distance which in effect reduces the magnification which is also undesirable.¹¹

In electron microscopes the lenses often use magnetic fields to bend the path of the electron. Ions, which travel slower and are much

more massive, would require much higher magnetic fields which are difficult to generate. For this reason ion lenses are generally electrostatic and consist of two very precisely machined washer shaped electrodes at some high potential.¹² The beam passes through the center of these concentric electrodes and is deflected and accelerated by the electric fields. The lens like operation is a result of the structure and fields which are cylindrically symmetric about the axis of the beam, and because the deflection of the beam by the electric field is proportional to the distance from the axis. One of the properties that limit the operation of a simple optical lens is chromatic aberration. This is when the lens has a different focal length for different wavelengths of light.⁴ Similarly, an electrostatic lens has a focal length which depends on the energy of the ions. The most serious practical limitation to the performance of most FIB columns is the chromatic aberration. To achieve high spatial resolution the optical column is designed to minimize chromatic aberration in the lenses.⁴ Because of the very high current density at the surface of the LMIS, the ion beam has an energy spread of five electron volts or more. As a result, the limiting design factor in the column is chromatic aberration rather than a spherical aberration.¹²

The use of electrostatic lenses focuses ions emanating from a point source to a point on the sample. This point can be deflected over a chosen area which is about 200x200 μ m. This deflection is what gives the FIB the ability to deliver a given dose in desired patterns on the

surface. This is done by deflecting the beam as well as being able to turn it off and on and align to existing features. Beam deflection is accomplished by a transverse electric field generated by electrodes.

(Figure 2-6) Parallel plates or octopoles are typically used for this. The deflection capabilities are responsible for some of the system limitations such as writing speed and field size.¹² If a transverse electric field V_x/d_0 acts on the beam over a distance L and an ion of mass m , charge e , and axial velocity v_z , then simple classical mechanics permits one to derive an expression for the angle of deflection θ .⁴

$$\theta = \frac{eV_x L}{d_0 m v_z^2}$$

If the ion has been accelerated by a voltage V_z , then $eV_z = mv_z^2/2$.

This yields⁴:

$$\theta = \frac{V_x L}{2V_z d_0}$$

It is important to note that the energy spread ΔE of the ions will lead to a

$$\frac{\Delta x}{x} = \frac{-\Delta E}{eV_z}$$

smearing of the beam in the direction of deflection.⁴

Equally important to deflecting the beam is the ability to shape the beam using a stigmator. The stigmator adjusts the shape of the beam by applying voltages to the deflector plates, the more the better, in the

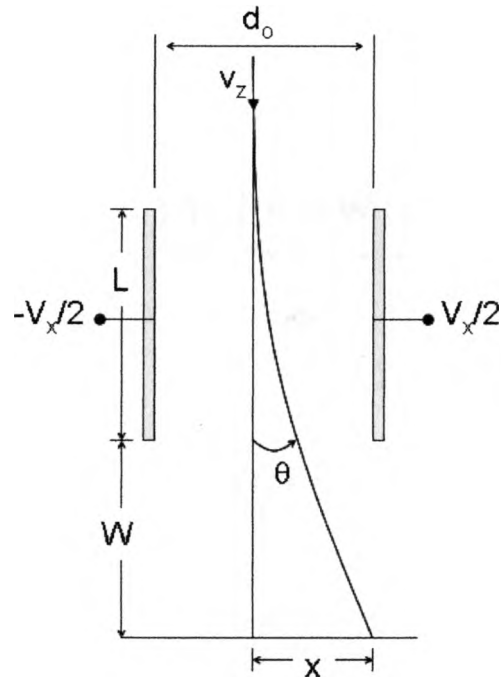


Figure 2-6: Beam deflection.⁴

focusing column. This effectively removes any shape irregularities, astigmatism, from the beam. This improves the spot shape on the sample surface resulting in clearer images and improved milling.^{7,12}

In addition to deflection it is important to be able to turn the beam off and on. This is an essential part of milling and is referred to as beam blanking. This occurs before the deflection plates. Blanking is done by deflecting the beam above an aperture preferably where the beam has a cross over. (Figure 2-7) The beam blanker deflects the beam perpendicular to the beam path. The beam is displaced laterally before sweeping it off the aperture resulting in tails in both time and space.⁴

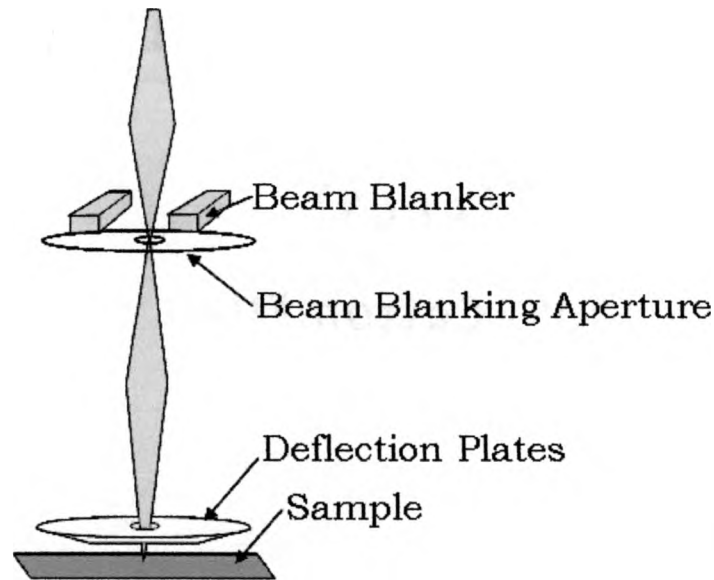


Figure 2-7: Simple image of beam with Beam Blanker and Deflector^{9,12}

The blanking pulse rises fast from zero, the initial beam path, and returns quickly to zero to minimize the tail.⁴

2.1.3 ION - MATTER INTERACTION

At the surface there are a number of actions that occur either independently or simultaneously of each other. (Figure 2-8) The main effects are implantation, damage, chemical changes in the sample, sputtering, ion induced deposition, ion assisted etching and electron emission. Each of these can be exploited in one way or another. Of these, electron emission, sputtering, ion induced deposition and ion induced etching will be discussed.

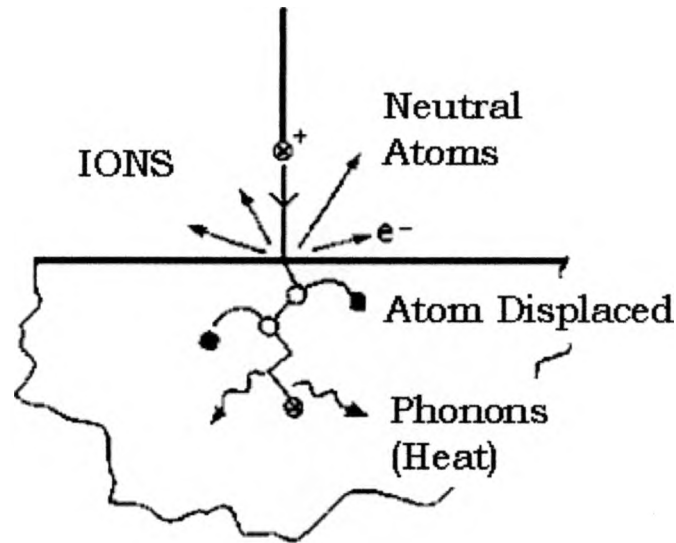


Figure 2-8: Ion - Matter interaction.³

Electron emission can be used to image the sample and therefore a key factor in the milling process. The electron emission occurs when the energetic ion is incident on the surface. The electrons have an energy distribution peaked at a few eV even though the ions may have many keV of energy.⁴ For each incident ion there are about 1-10 electrons emitted.³ The electrons are used in imaging of the sample with the

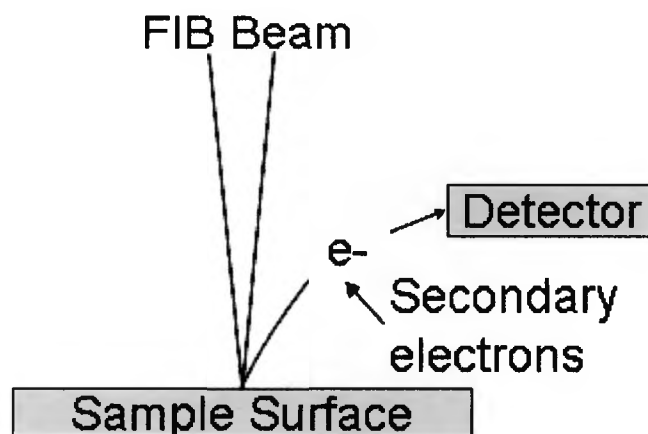


Figure 2-9: Emission of Secondary Electrons for Imaging¹⁴

focused ion beam in the same way that the secondary electrons are used in a scanning electron microscope. This can also be referred to as a SIM. (Figure 2-9)

Sputtering occurs when incident energetic ions cause atoms to be ejected from the surface leading to an erosion of the surface. This is also

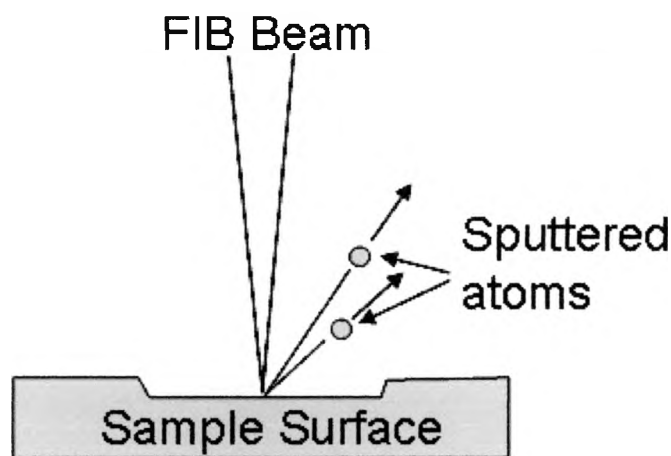


Figure 2-10: Ion Beam Milling ¹⁴

referred to ion milling. (Figure 2-10) This is a technique used in various forms of micromachining such as mask repair, circuit repair, I-beam lithography and MEMs manufacturing to name a few.³ This practice is also widely used in failure analysis and SEM and TEM sample preparation. The erosion can be controlled with very high resolution and it is possible to mill trenches with dimensions as small as 20nm. The milling yield generally increases as the angle of incidence goes from perpendicular to a glancing angle. This is often used to increase removal rate.⁴

Sputtering occurs at low energies 50-1000eV. The number of atoms removed per incident ion increases up to an energy of 1000keV before it begins to decrease. Typical yields are 2 to 30 atoms per ion. The atom leaves the surface with a few eV of energy. (figure 9) The total sputtering yield for a normal angle of incidence can be calculated using the Sigmund theory.¹¹

$$Y_{tot}(E_0) = \frac{4.2 \times 10^{14} \alpha S_n}{U_s} \quad [\text{target atoms/primary ion}]$$

U_s is the surface potential and

$$\alpha = 0.15 + 0.13 \frac{M_2}{M_1}$$

and

$$S_n = 8.462 s_n \frac{M_1}{(M_1 + M_2)} \frac{Z_1 Z_2}{(Z_1^{2/3} + Z_2^{2/3})^{1/2}}$$

where M_1 is the mass of the ion, M_2 is the mass of the atom, Z_1 and Z_2 are the atomic numbers and:

$$s_n(\varepsilon) = \frac{0.5 \ln(1 + \varepsilon)}{\varepsilon + 0.14 \varepsilon^{0.42}} \quad \text{and} \quad \varepsilon = \frac{32.53 M_2 E [keV]}{(M_1 + M_2) Z_1 Z_2 (Z_1^{2/3} + Z_2^{2/3})^{1/2}}$$

To find the yield for an ion at an angle of incidence θ

$$Y(E, \Theta) = Y(E) t^f e^{-S(t-1)}$$

Where f is the mass ratio of the target to projectile M_2/M_1 , $t = 1/\cos\theta$.

This was proposed by Yamamura and measured by Crow in 1990.¹¹

This lead to the finding that the sputter yield reaches a maximum near 80° and then reduces quickly as the angle approaches 90° .¹¹

Sputter rates can be increased by introducing a gas that will react with the surface into the milling process.¹ (Figure 2-11) This is referred to as enhanced etch. This is an operation in which a reactive compound is directed toward the surface of the sample while milling it with the ion beam resulting in faster milling rates and less redeposition. This is believed to reduce the redeposition of the sputtered material during the milling process. The use of a reactive gas can increase the removal rate

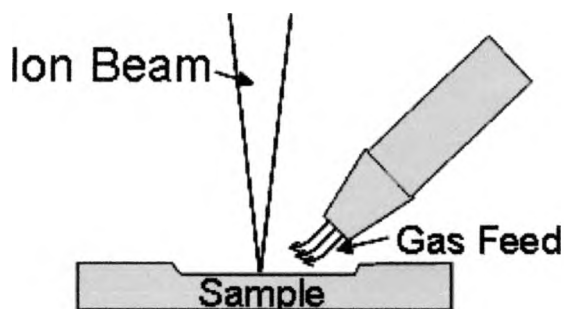


Figure 2-11: Gas enhanced etching.¹⁴

about 10x over standard milling rates. This is especially effective when etchants that are highly selective are taken advantage of. This selectivity can improve etch rate deltas and promote etching of a specific material leaving desired features.⁴

Another use of a gas fed system is ion induced deposition. The method is similar to that of enhanced etching but rather than acting on the sample the ions react with the gas causing a material to precipitate

on the sample surface. The gas is referred to as precursor gas atoms. For deposition to occur the beam energy is turned down below the

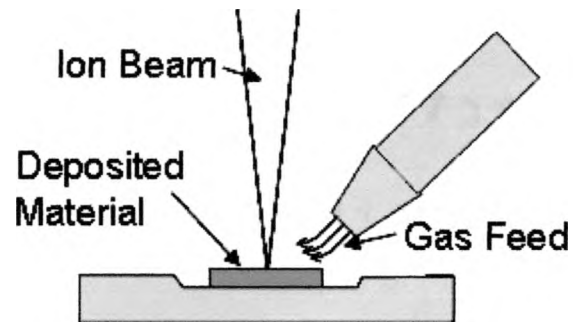


Figure 2-12: Ion Enhanced Deposition.¹⁴

point where sputter rate exceeds the deposition rate. An example of ion enhanced deposition would be the introduction of $W(CO)_6$. This is adsorbed onto the surface. The ion beam causes the gas molecules to disassociate leaving the W behind as a metal layer.⁴ (Figure 2-12) It is possible to use this method to deposit conductors for circuit rewiring, insulators (oxides), or protective layers for cross sections. This is particularly useful in circuit analysis and prototype work. Vias can be drilled and filled in the same tool as well as connections cut and others bridged making it possible to completely repair or rewire a circuit.^{4,6}

2.2 FOCUSED ION BEAM APPLICATIONS

The focused ion beam is one of the more versatile tools available on the market. All of these methods, imaging, sputtering, ion assisted etching and ion assisted deposition have a variety of applications. In this

chapter, the aforementioned capabilities will be put to use. Integrated circuit failure analysis, sample preparation and circuit analysis will be reviewed in addition to micromachining.

2.2.1 INTEGRATED CIRCUIT FAILURE ANALYSIS

One of the more common uses of the focused ion beam system is failure analysis of integrated circuits. The FIB used in the area of failure analysis is the deprocessing of the integrated circuit (IC). This is the systematic process of removing the thin film layers of the die permitting more visibility and accessibility to areas below the surface where the failure has most likely occurred. Deprocessing is a critical step in the failure analysis process since improperly or hastily implemented deprocessing procedures can result in the loss of key pieces of information needed to understand the physical cause of failure.² Traditional deprocessing techniques consist of various methods such as wet or dry etching and cross sections which can damage the area of interest to the point where the defect is obscured in the noise. This is also true of the FIB however the deprocessing can be controlled more precisely when used by an experienced FIB operator. Due to the increasingly high number of interconnect layers and increasingly small feature sizes, deprocessing has become quite a complex process requiring a high degree of skill. An added benefit to the FIB is that it is possible to do inline inspections without having to sacrifice a whole wafer. Modern

FIB's will load wafers up to a 300mm wafer allowing in-line investigations of failures and device characterizations.

2.2.2 CROSS SECTIONING

Table 2-1 reviews various methods of cross sectioning and their applications.² The ability to get down to defects that are less than 0.5 μ m is the reason the FIB has become the preferred tool for cross section preparations. These samples are then used in the SEM or TEM for

Sectioning Technique	Precision (microns)	Typical F/A Uses
Packaged-unit sectioning: Sawing	2000	Gross internal package problems Ceramic Packages
Packaged-unit sectioning: Grinding	500	Assembly problems
Wafer cleaving: Manual	1000	Repeated structure or layer problems
Wafer cleaving: Precision	1.5	Localized structure or layer problems
Die Polishing	0.2	Device defects > 0.5 microns
Focused Ion Beam: Sectioning	0.05	Surface defects or defects < 0.5 microns
TEM sample preparation techniques	0.05	Defects < 0.5 microns requiring high resolution imaging

Table 2-1: Precision and uses of various cross sectioning techniques.²

imaging. In a dual beam SEM-FIB the sample can be viewed without ever removing the sample. This improves throughput and reduces the time required to find answers translating into higher earnings.

A cross section is one of the most useful tools for failure analysis. The application of sputtering is an effective method for cross sectioning samples to look below the surface. The typical strategy is to image an area on the computer screen. Once the general location is found a box is

drawn using a computer mouse and processing software to represent the area to be cross-sectioned. The program can then scan over this area to

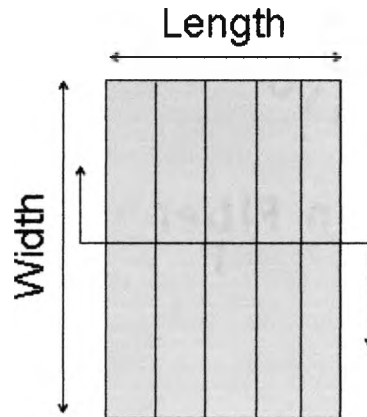


Figure 2-13: Coarse Mill Scan Pattern¹¹

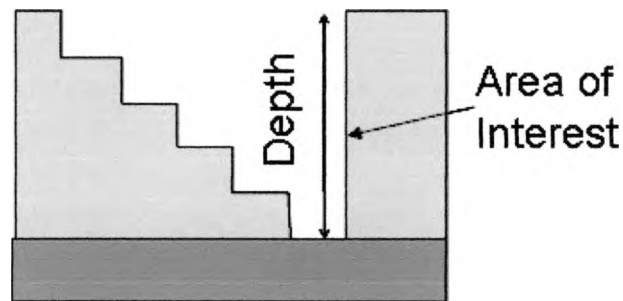


Figure 2-14: Coarse Mill Cross Section¹¹

deliver the specified ion dose as setup in the recipe consisting of the beam current and dwell time. The recipe will determine the beam energy, the dwell time and the step size.⁴ Figure 2-13 represents a coarse mill pattern. The initial cut is a rough cut made in a staircase pattern. (Figure 2-14). This is usually done at high energy levels to remove the bulk of the material and is in the shape of a staircase to give room for the redeposited material without adding noise to the area of

interest. A higher beam current can be used to reduce dwell time. If a large volume of material is to be removed an enhanced ion etch should be considered to reduce the mill time.

Following the coarse mill a clean up mill with a simple pattern, figure 16, is performed making the face of the area of interest easier to see. The clean up step happens in two phases. In the first step, the fine mill pattern should be the same width as the coarse mill pattern and should be just short of the edge of the area of interest. The beam current for this mill will be much lower and the dwell time should only be for 15-20 seconds within a range of 250-500pA. (Modern systems can adjust the time according to the beam current intensity.) The geometry of the existing sputter crater will cause the sputter yield to be much higher because of the non-normal angle of incidence.¹¹ The second step of the clean up is just like the first step however the pattern will just overlap the face of the area of interest. A longer scan time will be used for this mill but a much lower beam current, between 50-100pA, will be used with the same dwell time and overlap as the first step of the clean up. The results give higher resolution to the details in the area of interest, figure 2-16.

The results can be viewed by tilting the stage to 45° and using a very low beam current of 1-5pA and a very slow scan to enhance the



Figure 2-15: The fine mill pattern is a much smaller than the coarse mill pattern.¹¹

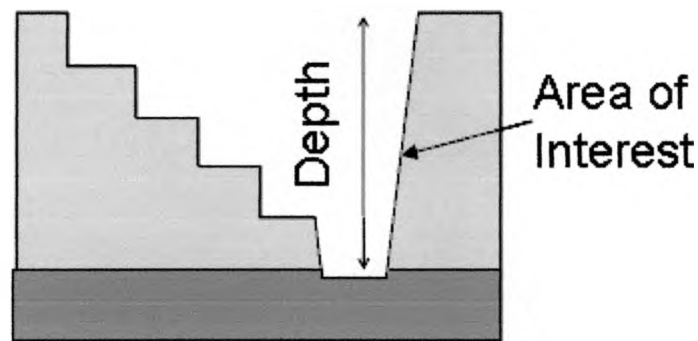


Figure 2-16: The fine mill cleans up the face of the cross section at the area of interest.¹¹

signal to noise ratio. It is important to make all focus and stigmation adjustments away from the area of interest so as not to damage that region. When using the secondary electrons for imaging the metals will be bright and the insulators will be dark. If secondary ions are used for imaging both metals and insulators will be bright. In general the secondary electron image will yield better results because more electrons will be emitted than ions. Figure 2-17 compares the various imaging

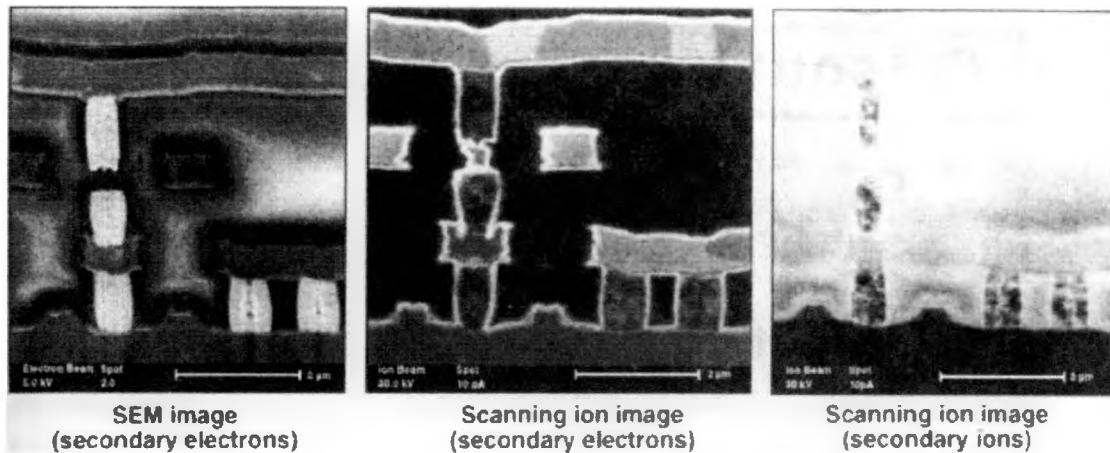


Figure 2-17: Comparison of various imaging techniques.¹¹

techniques. The SEM image is the most common form of imaging and is available on dual beam systems (SEM-FIB). The image of created using secondary ions has the lowest resolution.¹³

2.2.3 TEM SAMPLE PREPARATION

Using the same method, TEM (transmission electron microscope) samples can be prepared. The FIB has greatly simplified TEM sample preparation. No longer is micro-cleaving, mechanical polishing and broad ion beam thinning necessary. This process is the same as creating a SEM sample but in the case of making a TEM sample the two mills are done back to back leaving a thin sample, figure 2-18. The major concern of using a FIB for sample preparation is the damage caused by the beam during milling. The damage inflicted usually manifests itself as a blending of regions of the sample which will increase diffuse scattering of the TEM beam limiting the amount of information that can be gleaned from the sample.

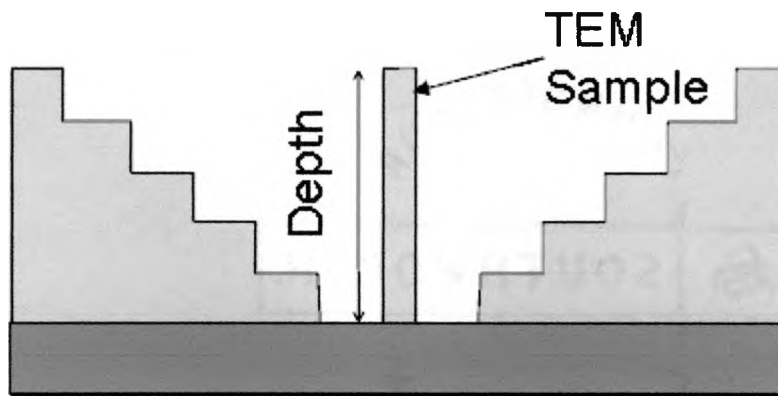


Figure 2-18: TEM sample preparation.¹¹

2.2.4 MICROMACHINING

Each of these techniques can be forms of micromachining and can be taken advantage of for numerous applications. Micromachining is used in MEMs manufacturing, ion beam lithography, electrical sample preparation, mask repair for lithography and circuit repair which will be discussed in more detail in chapter 3.

2.3 DUAL BEAM SYSTEMS

A dual beam system, or a dual column, refers to a SEM-FIB system. The enhanced capabilities of a dual beam system provides all the capabilities of a SEM and FIB in a single system simplifying many of the standard FIB applications. As with FIB systems, SEMs have been used extensively in the semiconductor industry. These are the tools of choice for defect review and process monitoring. The non-destructive

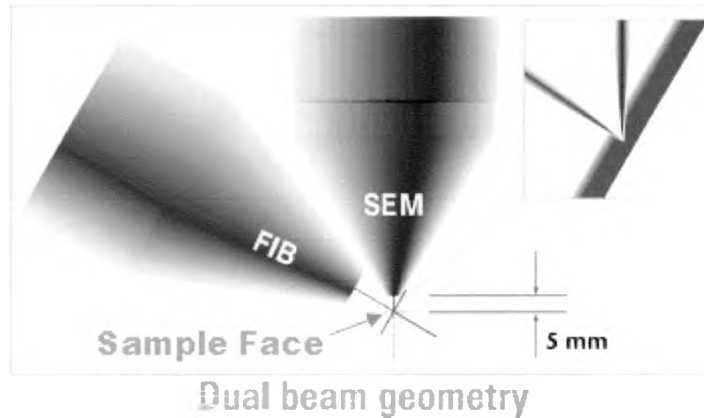


Figure 2-19: Dual Beam System¹²

nature of the SEM and the high resolution imaging makes it well suited for these tasks. Where the SEM is lacking is in the ability to characterize buried defects and is limited to 2D analysis and metrology. These limitations prompted the development of the dual beam system.⁵

A well designed dual beam system is able to integrate the ion beam's milling and deposition capabilities with the electron beam's high resolution, non-destructive imaging without compromising the performance of either column.⁵ This integration increases throughput and enables real time analysis in the line.

Traditionally the deposition of metals and insulators has been done using the ion beam. This has mainly been used to connect or isolate metal lines in a circuit for device modifications. With the dual beam system it is possible to deposit a metal over smaller particles or defects without damaging the object of interest with the electron beam. For defects less than $0.2\mu\text{m}$ the ions used for depositing will damage defect during the initial exposure. Once the initial layer has been

deposited with the electron beam the remaining amount can be deposited with the ion beam.⁹

CHAPTER 3

SAMPLE DATA AND ANALYSIS

3.1 OVERVIEW OF SETUP

3.1.1 THE TOOL

The primary tool used for these experiments was the FEI xP DualBeam Workstation. This tool was equipped with a Magnum column (shown in Figure 3-1) and the LMIS for these tools was gallium. For added

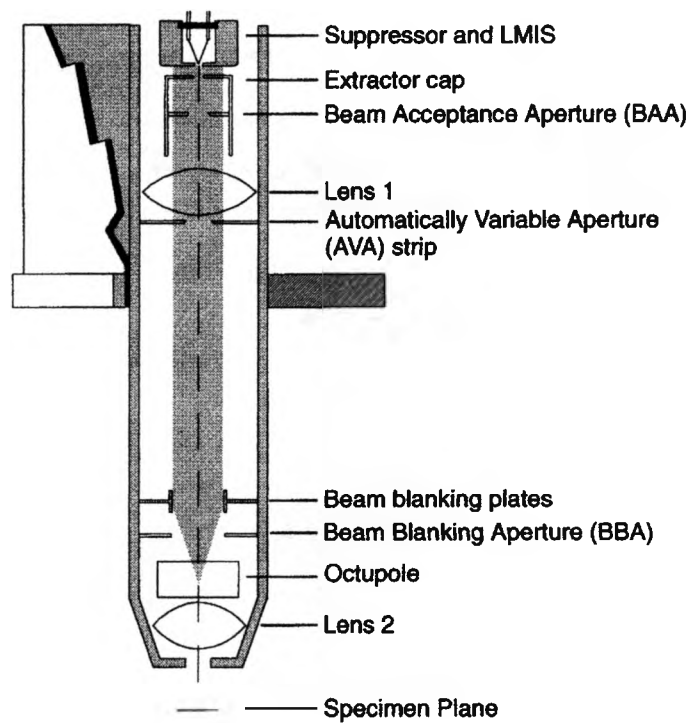


Figure 3-1: FEI's Magnum Column¹²

convenience the tool was also supplied with an optical microscope in the chamber. The platinum deposition experiment was performed on a previous generation tool, the FEI DualBeam 820. (Throughout this chapter all descriptions and instructions will be for the xP system except for the section describing deposition which will only refer to the operations necessary for this application.) Access to both tools was granted by Philips Semiconductors. The systems were of similar design however the xP workstation had improved operating software that made TEM sample preparation less cumbersome.

3.1.2 FOCUSING AND BEAM SETUP

Modern systems are becoming more and more user friendly. With today's software controls, loading and setting up a sample is a relatively simple task. Setting up the beam and column, on the other hand, takes a little practice.

Once the sample is loaded the optical microscope is used to find the area of interest. Start by turning on the beams. The HV (high voltage in the column) should move to 30kV and the ion emission current should be about 2.5 μ A. The V/I slope should be 103.3 V/ μ A. If the ion emission current is too high the suppressor is used to lower or raise the current. If there is no response the extractor is used although not recommended. This will only be necessary if the tool has been idle and the tip needs heating. If the extractor is adjusted the beam needs to be realigned so it is best to do this at the beginning of a session before the

beam has been aligned. The forward working distance is set to 5mm initially although this will be manipulated during the eucentric focus. Next a detector is selected to obtain an image. On the xP system there are two basic detectors, the TLD (Thru-the-Lens Detector) and the CDM/CDEM (Continuous Dynode Electron Multiplier). The TLD is better if the sample is not charging because of the better signal to noise ratio.¹² The CDM is a side mounted detector that offers a side view of the sample which is helpful in looking at topography that might be missed in a top down view.¹³ Typically the beam of choice, initially, is the electron beam so as not to damage the sample during the setup. Once the beam is selected the scan rate and resolution need to be set. This is generally set to a medium resolution and a fast scan rate so the image is refreshed more often making it easier to see how the adjustments are affecting the image. The contrast and brightness are corrected with the adjuster to clean up the image. Finally the focus and astigmatism is adjusted to get the final image.

There are three modes of image resolution available with the E-beam. They are search mode, ultra high resolution mode (UHR) and energy dispersive X-ray (EDX) mode. Search mode is the default resolution and is used for wafer alignment and navigation. This is a low magnification setting. The UHR mode is applicable to most imaging and analytical operations when the magnification needs to be more than 1000 to 2000 X. The immersion lens is turned on for this setting and the

TLD is used to form ultra high resolution electron images of the sample. If UHR is used for the I-Beam imaging, the final lens is turned off to allow imaging to take place with the last selected detector. The EDX mode is used to reduce backscatter for cleaner spectra when using the X-ray option.¹³

Optimizing the image is as much an art form as it is science and improves with experience. The image can be optimized by changing scan speeds, focusing, stigmating, adjusting the spotsize or changing the magnification. The highest quality images are generally obtained by using slow single scans with a low beam current. If an image is noisy with No Averaging (a software setting) selected the scan speed can be reduced to improve the image quality by increasing the signal to noise ratio. Image quality also improves using averaging.¹³

Focusing is the first option for improving an image once the optimum scan speed has been selected. The easiest way to get the best focus is to find a feature that has distinct edges. Use a combination of brightness, contrast, magnification and stigmatism to maximize the image quality. This is usually done at very high magnification, typically 2X to 3X the working magnification, so that all reduced magnifications are also in focus. If focusing while using the I-beam, move away from the area of interest so it is not damaged by incidental milling.¹³

Correcting the astigmatism will need to be done each time the aperture or working distance is changed (known as stigmatism).

Astigmatism is caused by imperfections in the optical system resulting in elliptically shaped features in the image and is usually only noticeable at higher magnifications of 3000X or more. If astigmatism is present, the result is a directional distortion change of 90° between the two out of focus conditions.¹²

To improve the image even further it is important to adjust the E-beam spot size to the point where the edges of the beam just touch when adjacent lines are scanned. When the spot size is too big it will overlap making the image appear out of focus. If the spot size is too small then the image is cluttered with electronic noise. A smaller spot size is used for higher magnifications and a larger spot size is used for lower magnifications. The spot size can be selected from a drop down menu of presets through the software on this tool.

The I-beam aperture and current settings are important for getting the desired results during milling and imaging. In general a smaller aperture is used for high resolution imaging and a larger aperture for faster milling. Depending on the application, the I-beam current can be set anywhere from 1pA to 11500pA. Table 3-1 lists some recommended beam currents.

Working with the magnification on a FIB or a SEM is a little more complicated than with an optical microscope. On the FEI tool there is a selection of predefined magnifications. When the magnification is

Beam Current	Uses
1 pA	<ul style="list-style-type: none"> • Very high resolution imaging • High aspect ratio holes • High resolution imaging • Pt via filling
10 pA	<ul style="list-style-type: none"> • Quick imaging • Fast Pt via filling
30, 50 pA	<ul style="list-style-type: none"> • Navigation imaging • Milling submicron holes • Final milling on cross sections
100 pA	<ul style="list-style-type: none"> • Milling micron-sized holes • Intermediate/final milling on cross sections • Short Pt strap deposition
300, 500 pA	<ul style="list-style-type: none"> • Milling micron sized holes • Medium Pt strap deposition • Intermediate milling on cross sections
1000 pA	<ul style="list-style-type: none"> • Initial milling for small cross sections • Long Pt strap deposition
3000 pA	<ul style="list-style-type: none"> • Initial milling for medium cross sections • Longer Pt strap deposition
5000 pA	<ul style="list-style-type: none"> • Initial milling for medium large cross sections • Pt probe pad deposition (40μm x 40μm)
11500 pA	<ul style="list-style-type: none"> • Initial milling for large cross sections • Pt bond pad deposition (50μm x 50μm)

Table 3.1: Recommended Beam Currents¹³

decreased there may be a dark or bright square in the center of the screen. This is from charging when using the I-beam. Even the slightest modification of charging samples and the effects of sputtering or gallium implantation are readily apparent in the image.

The automatically variable aperture (AVA) automatically adjusts the effective beam defining aperture to vary the beam current and arrive at the effective aperture desired. The SEM AVA is the electron column apertures used for different imaging needs. The SEM AVA aperture strip contains four different-sized heated apertures. (Other tools may have a

different number of apertures.) Table 3-2 is a list of recommended apertures and uses. If many apertures selections have been made it may

Aperture	Use
2000 μm	Service only, for alignment
70 μm	X-ray dot maps
50 μm	X-ray mapping of low-Z elements at low kV
30 μm	For general use and high resolution imaging

Table 3.2: SEM AVA Aperture Recommendations¹²

become necessary to home the SEM AVA to remove any accumulated error. This will cause the AVA to drive to the home position and return to the selected aperture position.

3.1.3 THE EUCENTRIC POINT

The most critical step to getting clear images with the I-beam and clean cuts during milling was getting the eucentric height set correctly. This is very important and, to the beginner, very challenging. The eucentric height needs to be adjusted after loading any new sample. In addition to getting better images and cleaner cuts, getting the sample set to the eucentric point, the various components of the workstation (GIS, EDX and SIM) can be used safely. It is not as likely for the components of these to be damaged by the sample.

The eucentric point is where the stage tilt axis and the ion electron beam axes intersect. At this point, the point of interest will remain in focus and almost no image displacement occurs regardless of how the stage is tilted or rotated. The excerpt from the FEI operations manual

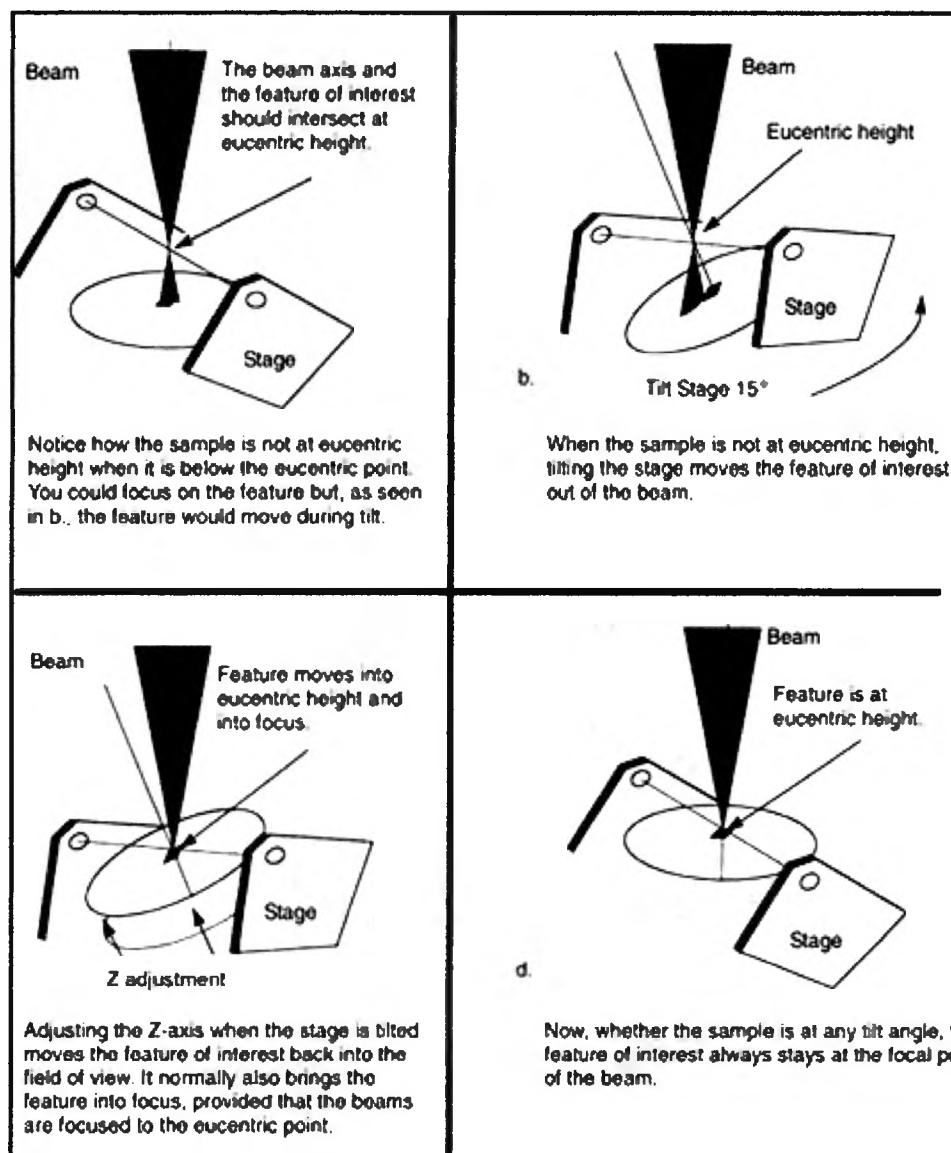


Figure 3-2: Eucentric Height Described¹³

(Figure 3-2) explains in more detail the eucentric height. Finding the eucentric height is done manually and requires an E-beam working distance of approximately 5mm. To start with the electrical beam shift is set to zero (this is used at high magnifications rather than stage movement) and the stage tilt is set to zero. Next an image is acquired with the E-beam. The image is brought into a coarse focus with the z-control which moves the stage up and down. Once a rough focus is found the image is magnified 1000X until a distinct feature is found which is centered under the crosshairs at the center of the screen. The stage is then tilted to 15° while watching the object under the cross hair to see what direction it moves. The z-control is used to bring the object back under the cross hair. This is repeated for 45°. Once this is completed the stage tilt is returned to 0° while verifying the object remains under the cross hairs. If it moves more than 5-10µm it will be necessary to repeat the alignment. When finished this height is stored into the software for reference by all other movements within the system. Once the eucentric height is found for the E-beam it is necessary to align both beams to the eucentric height. Begin by tilting the stage to 52°. Next find a distinct feature (usually the same feature is used from the previous steps) and magnify 1000X and center it under the crosshairs. Once the object is centered, switch to the I-beam. The image shift is used to bring the object back under the cross hairs. If the image can not be found then eucentric height will most likely need to be found again. If

the object selected was small and not readily bound to the surface it is possible that the ion beam dislodged or milled it away and it will be necessary to select another feature.¹³

The free working distance (FWD) is measured from the lower end of the stage drive up to the sample holder. The working distance is the distance from the nose cone of the focusing column to the sample surface or from the bottom of the final lens to the sample surface. This is calibrated by setting it equal to the Z value determined by finding the eucentric point. Once this has been done the changes in the stage height are subtracted from the current FWD value and the final lens of the electron column is automatically refocused to the new stage height.¹³

This process was rather long and tedious but essential to good data collection. Each time a sample was loaded the sequence had to be repeated. However, once the beams were aligned and the tool is in shape it is time to put the tool to work.

3.2 SAMPLE 1 – FAILURE ANALYSIS OF AN INTEGRATED CIRCUIT

The first sample evaluated was a test structure from the scribeline of an ASIC device that failed electrical testing. The die was on an eight inch wafer that was donated by Philips Semiconductors. First the failure was identified electrically and then by isolating the failed structure architecturally it was possible to FIB the specific location. A schematic of various scribe line process control modules (PCM's) was referenced to find the electrical layout of the structure. By identifying the failure as a

the defect location. A staircase pattern, site 2 in Figure 3-4, was used with a beam current of 1000pA. During the coarse mill much of the oxide was redeposited in the corners.

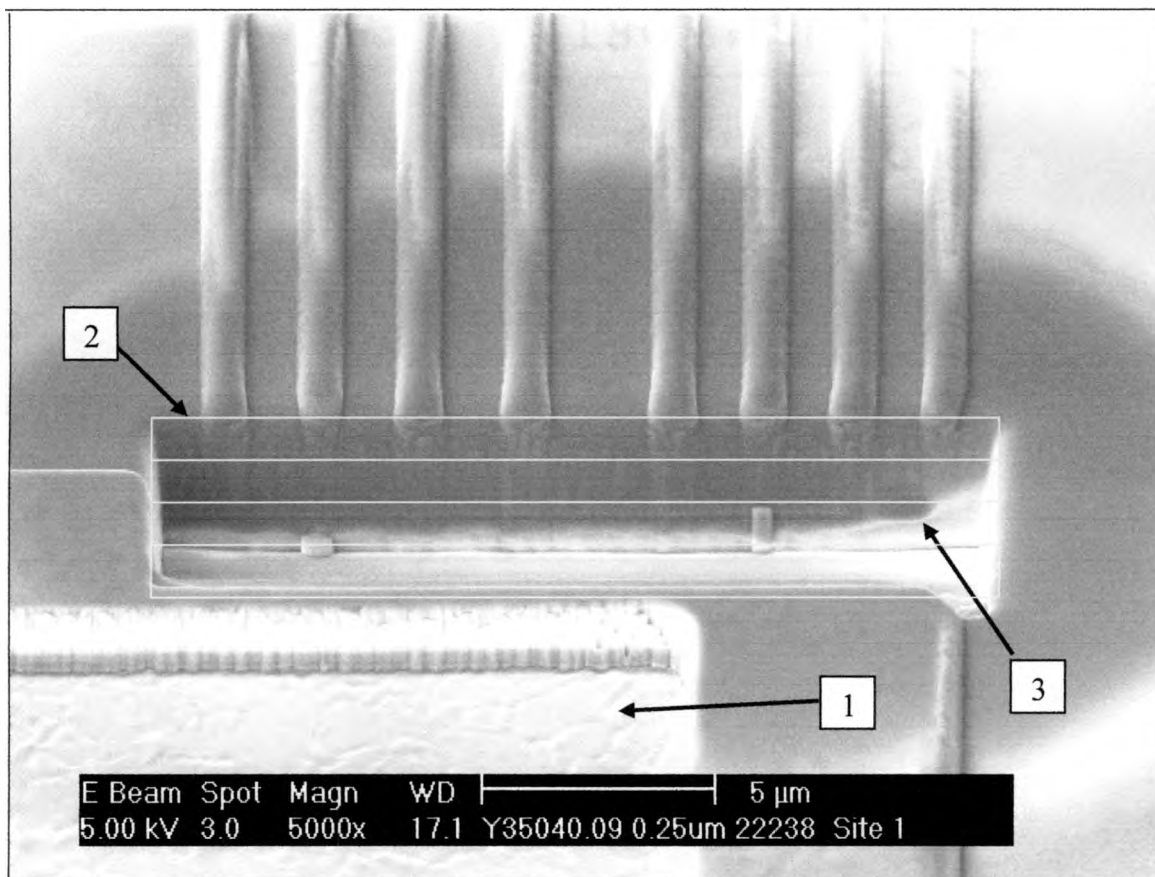


Figure 3-4: Site of Failure Post Coarse Milling. 1) area of first mill attempt 2) mill pattern 3) redeposition or “slag”

Once the coarse milling was completed a fine mill was used to clean up the area of interest removing the debris from the coarse mill. The fine mill was done at 500pA. The results can be seen in Figure 3-5. Notice that the mill went much deeper and the difference in etch rate highlights the metal lines.

Figure 3-5 shows that several of the metal lines were not formed or formed poorly. By making this discovery the information was fed back to the etch group who later found a problem with one of the etchers. Actual

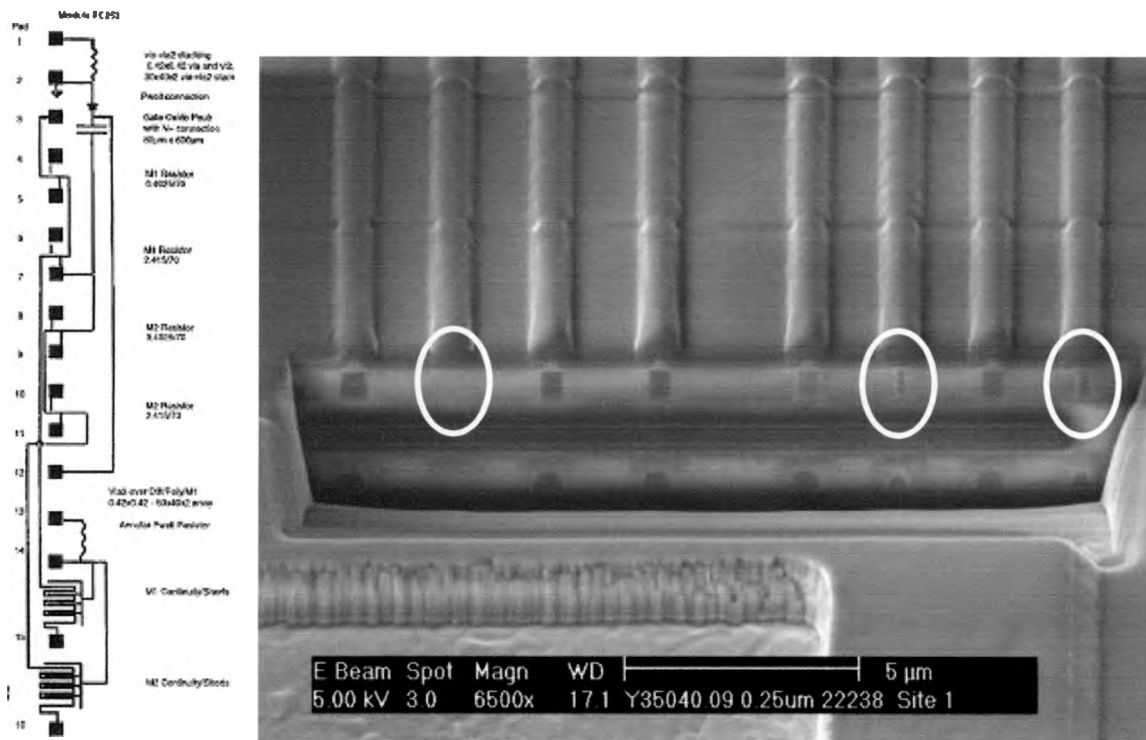


Figure 3-5 M2 - M2 Continuity Failure

work time to make the discovery took about one hour. Under normal circumstances this would have been at least a half day project allowing for cross sectioning, sample lapping getting to the failure and then SEM the sample.

Overall this project went as planned with the exception of a couple of beginner mistakes. Site 1 in Figure 3-4 shows where the first coarse mill took place. By not having the two beams aligned correctly the target

was missed. This was a lesson learned not to hurry on sample setup which served well on the next sample.

3.3 SAMPLE 2 – MATERIAL DEPOSITION

The next sample was a wafer donated by Philips Semiconductors. The investigation was to determine if the metal lines were being formed correctly and to see the shape of the “top hats” at the end of the metal lines. In order to do this it was important not to mill too far into the sample otherwise the “top hats” would be damaged from the ion beam. To protect the area of interest, platinum was deposited on the surface to act as a shield to the underlying films.

The tool used for this test was the FEI DualBeam 820. (The primary FIB was down hard for beam control.) This tool is the predecessor to the xP system and with the upgrades on the tool differed only in some of the software options. The first step was to deposit the platinum over the area of interest. The Pt had to be heated prior to deposition which took approximately fifteen minutes. Once the heat cycle was completed the beam current was lowered to 70pA. A pattern was drawn around the area of interest and the material, platinum, was selected in preparation for deposition. Using the I-beam to image needle was inserted to the point of deposition. This has to be performed with extreme care or it is possible to drive the needle into the sample or leave it too far away resulting in a poor deposition pattern. After everything is setup the milling begins and Pt is deposited on the wafer in the shape of the

pattern. (Figure 3-6) With the platinum in place it was time to do the mill. The coarse mill was with the ion beam at 1000pA with 30kV followed by a fine mill for cleanup at 150pA. (Figures 3-7 and 3-8)

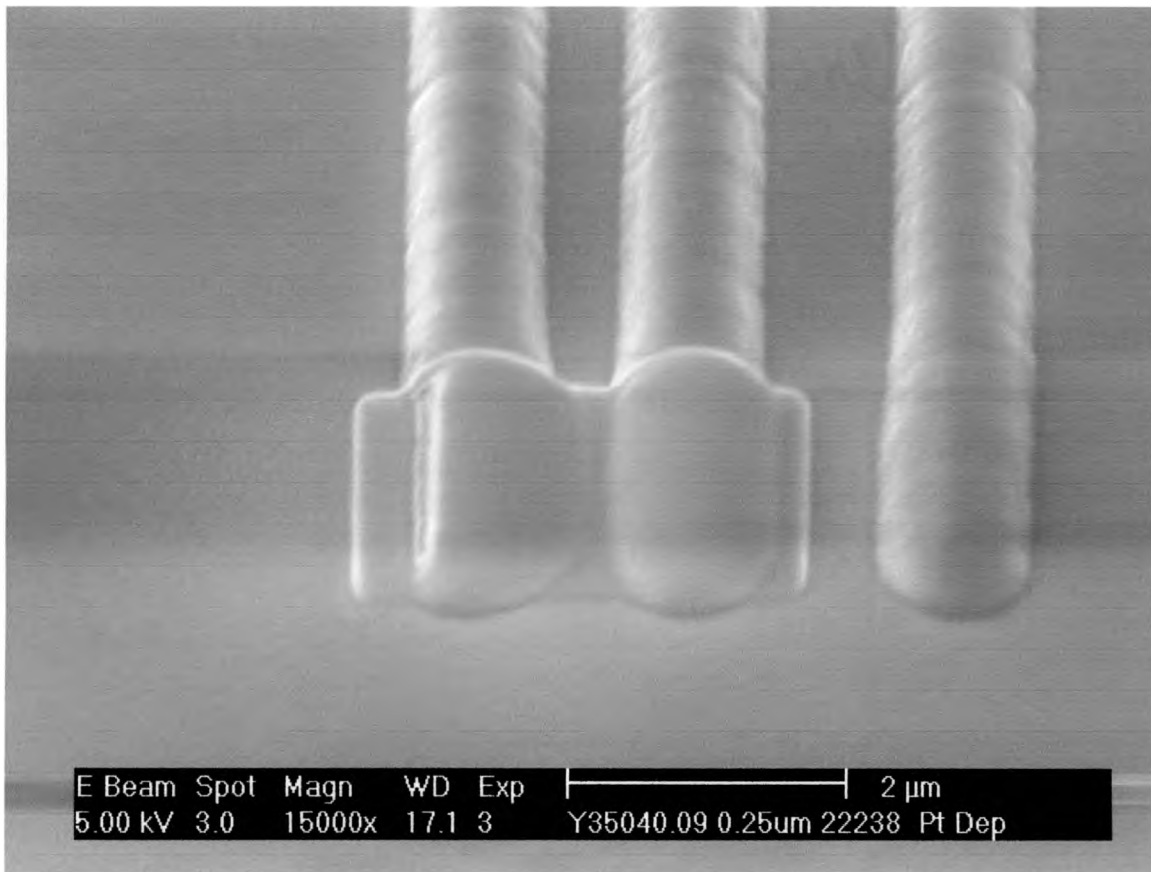


Figure 3-6: Platinum deposition

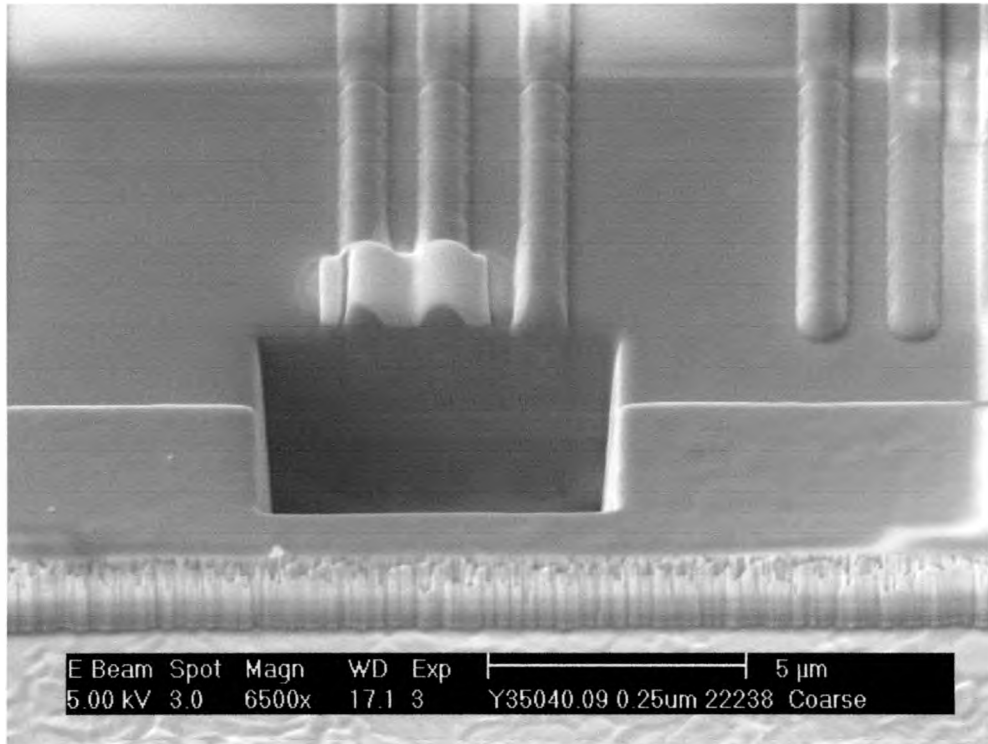


Figure 3-7: Coarse Mill

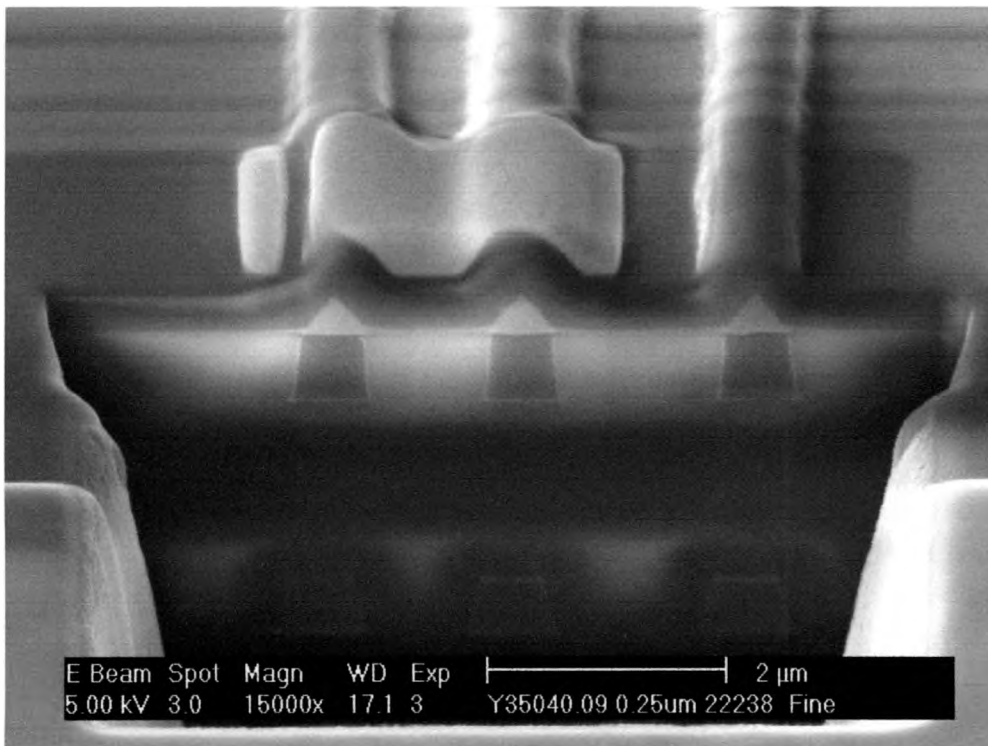


Figure 3-8: Fine Mill (Clean up)

This was a successful demonstration of how a material can be deposited and how it can serve as a hard mask to protect sensitive structures from the ion beam. Figure 3-8 shows that the Pt protected the underlying structures. With careful setup this test went according to plan. One thing that noticeable about the setup of this test was the bare area at the left of the Pt deposition. This is due to the placement of the needle and possibly the angle of the ion beam. In future designs it would be beneficial to be able to deposit without the stage tilt or to have the gas deposited from more than one angle.

3.4 SAMPLES 3 – 5 – MICROMACHINING

Samples 3 through 5 were various NiFe metallic films provided by Dr. Carlos Gutierrez. The objective was to machine different geometries into the metal to investigate the effects of the geometries on the magnetic domains. Each sample was approximately 1.5cm x 1.5cm. Each sample was to be quartered as shown in Figure 3-9. Micro wires in the upper

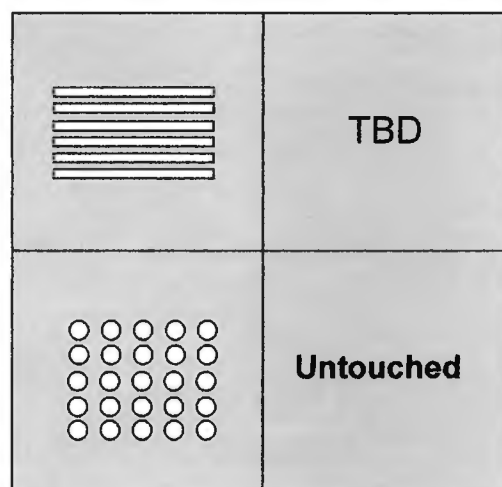


Figure 3-9: Example of Micromachining Layout

left corner and cylinders in the lower left corner. The lower right corner was to remain untouched and used as a reference. The upper right was for variations on different geometries such as serpentine structures, isolated wires, bridged wires or hexagons. Each of the following samples will refer to specific mills rather than specific whole samples.

3.4.1 Learning

Milling patterns into various materials is as much an art as a science. Developing a “feel” for the tool takes practice. Many of the instructions from the manual and the instructor are just a starting point as all samples behave differently. The ion beam can cause a lot of incidental damage if not used properly. Figure 3-10 demonstrates the

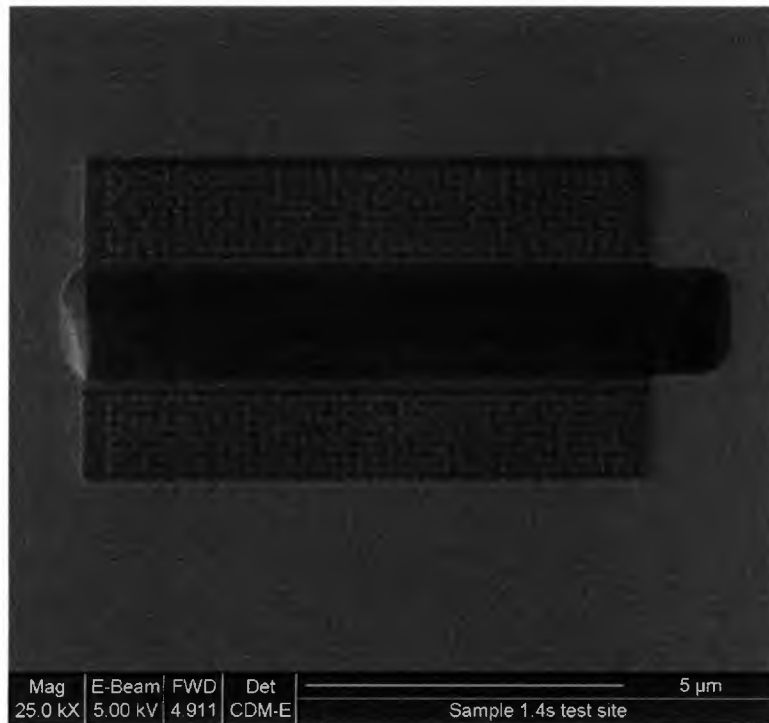


Figure 3-10: Example of Excessive Ion Beam Exposure

Effects of imaging with the ion beam for an extended period of time. During this mill the ion beam was used to image the results. During the period of inspection the skin layer of the sample was milled away. To prevent this in subsequent images a lower beam current was used. After some general practice of milling and imaging more complex patterns and milling techniques were experimented with. Of these, parallel milling, serial milling, high current and low current milling were tested. Depending on the pattern required each technique has its place. For the failure analysis requirements mentioned earlier the parallel milling with high beam current was most effective followed by a serial mill at low

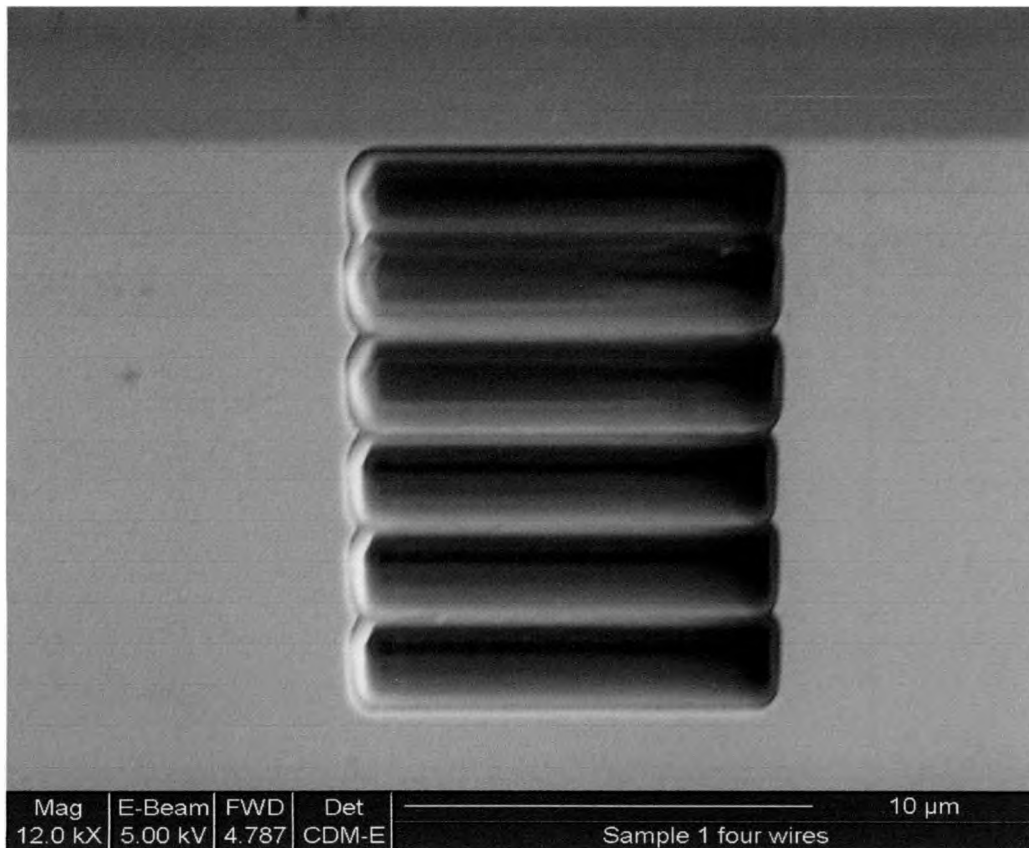


Figure 3-11: Example of parallel milling followed by a serial mill for cleanup. Beam current was 870pA with an emission current of 2.6 μ A.

current. When this technique was used for micromachining structures and patterns the results were less than satisfactory as can be seen in Figure 3-11. The wires that were milled were etched to a level below the sample surface. Following the mill of the wires another pattern was milled on either side to isolate the wires, Figure 3-12. The cuts were

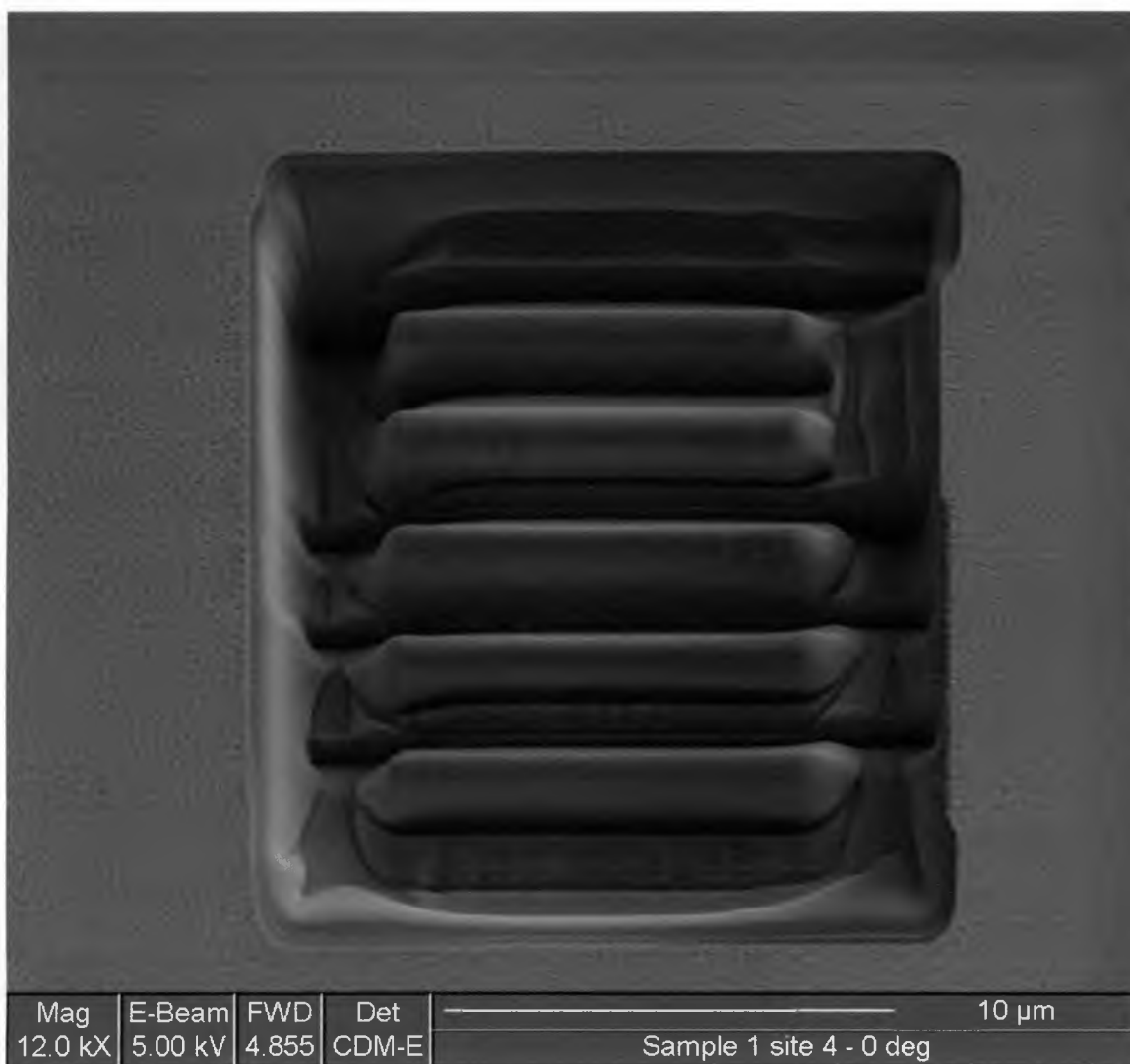


Figure 3-12: Final result of micromachining wires using the parallel method.

uneven and eroded the metal lines even more. In addition to the erosion, the wires were not adequately isolated. Also notable is the ion beam

damage around the structure from imaging with too high a beam current. In an attempt to improve the results of milling wires using the parallel milling method a higher beam current was first tested. The results can be seen in Figure 3-13.

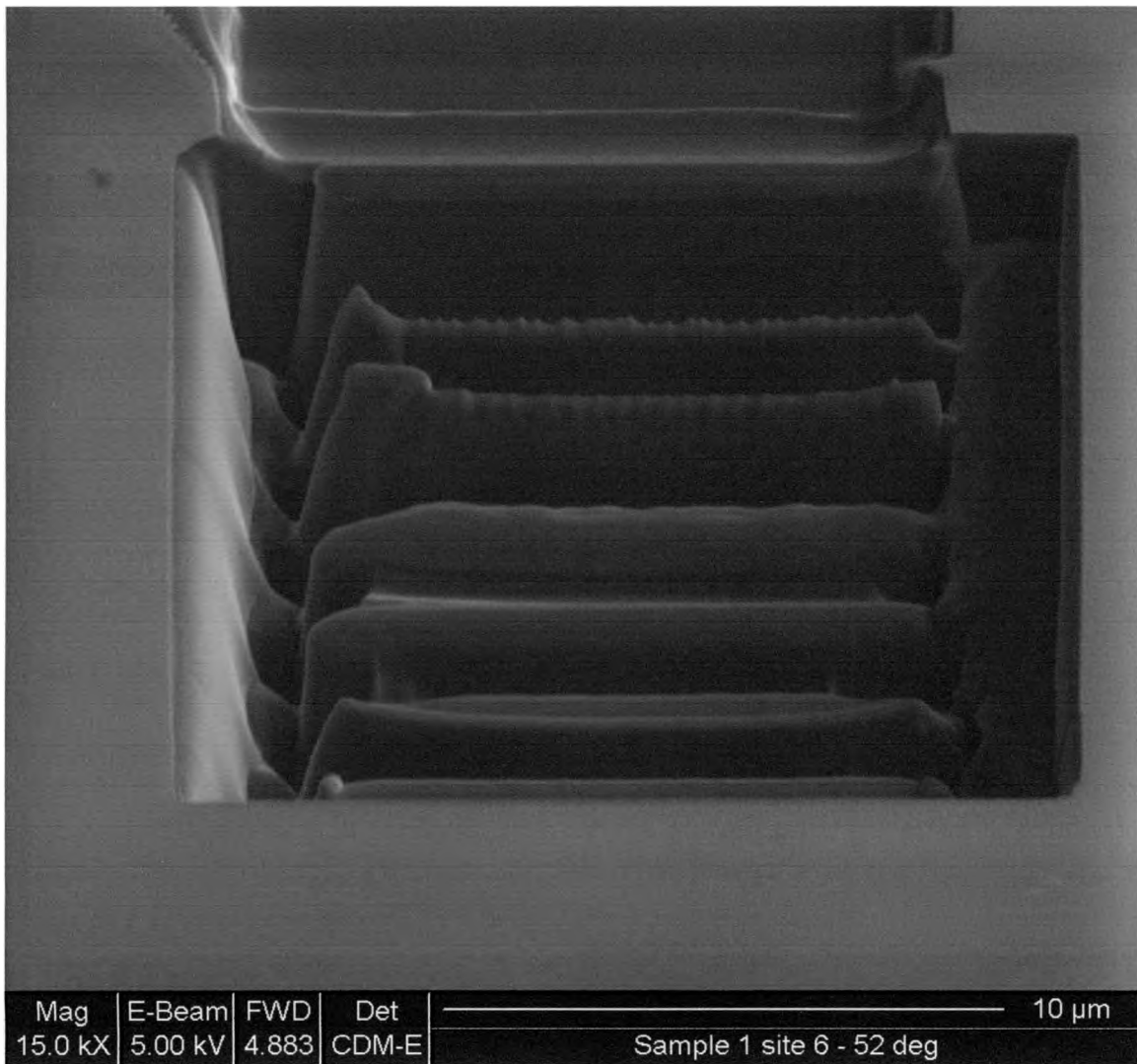


Figure 3-13: Milling wires with a higher beam current followed by a cleaning mill. Beam current 1000pA, Ion Emission 2.2µA for initial mill. Beam current of 500pA used for the cleaning mill.

Again, much of the material redeposited between the wires and the right. The initial cut was performed with a 1000pA beam current and 2.2µA ion

emission current. The clean up mill was at 500pA in serial mode. (Half of the initial beam current is generally recommended for the cleaning mill.) Several more attempts at machining the wires using parallel mode proved just as fruitless. Use of serial milling dramatically improved results (Figure 3-15). This mill was followed by the isolation mill seen in

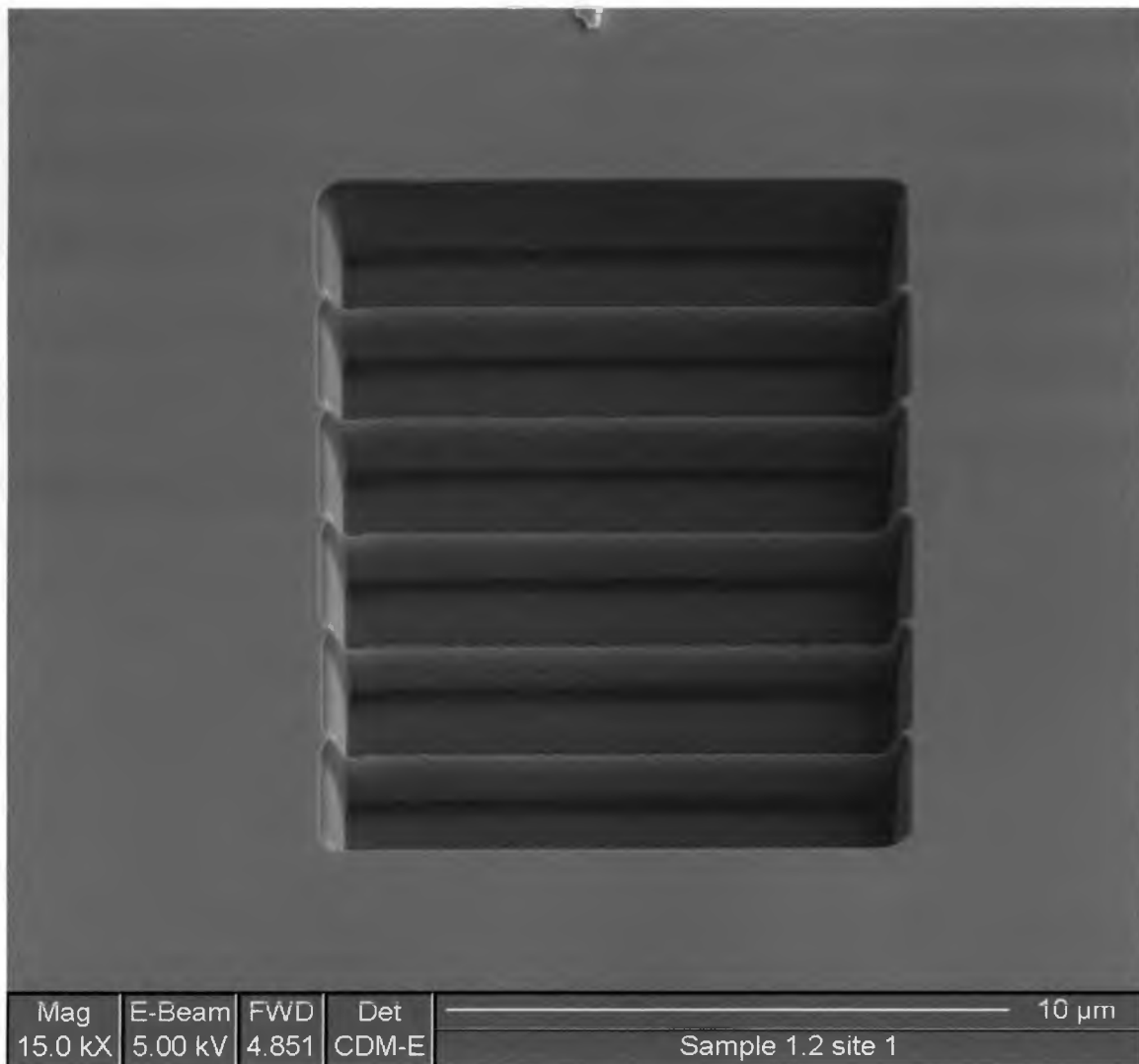


Figure 3-14: Use of serial mode for milling provides much cleaner lines without redeposition. Figure 3-15 where again the problem of redeposition caused problems.

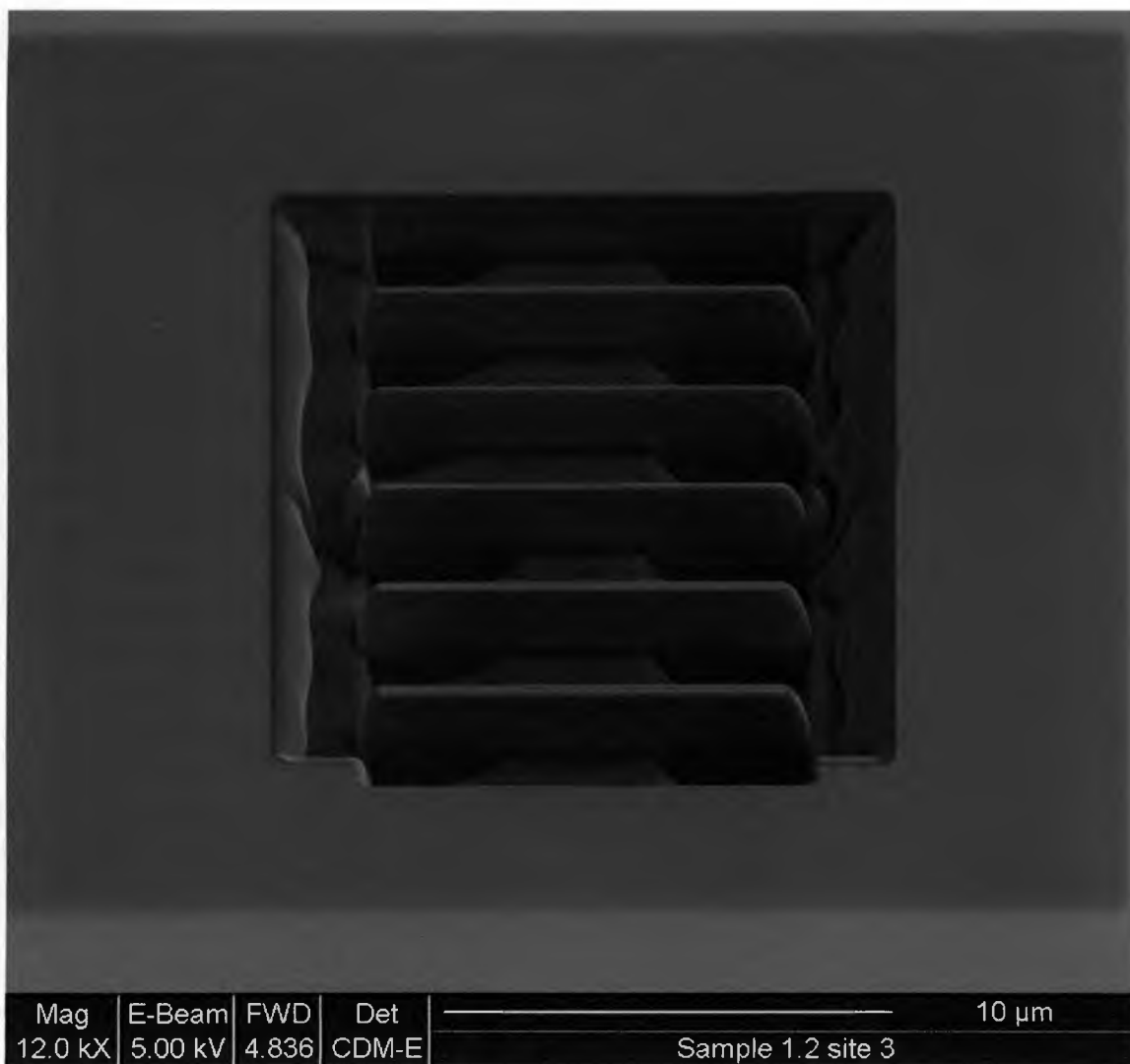


Figure 3-15: Serial mode milling for wire isolation proved to have similar redeposition problems.

Acceptable results were achieved finally after milling all areas at the same time using a serial mill seen in Figure 3-16. This proved to be very slow, approximately 10 minutes per mill. By milling all regions at the same time it was possible to use slightly higher beam currents, 850pA, than had been attempted previously keeping milling time under 20

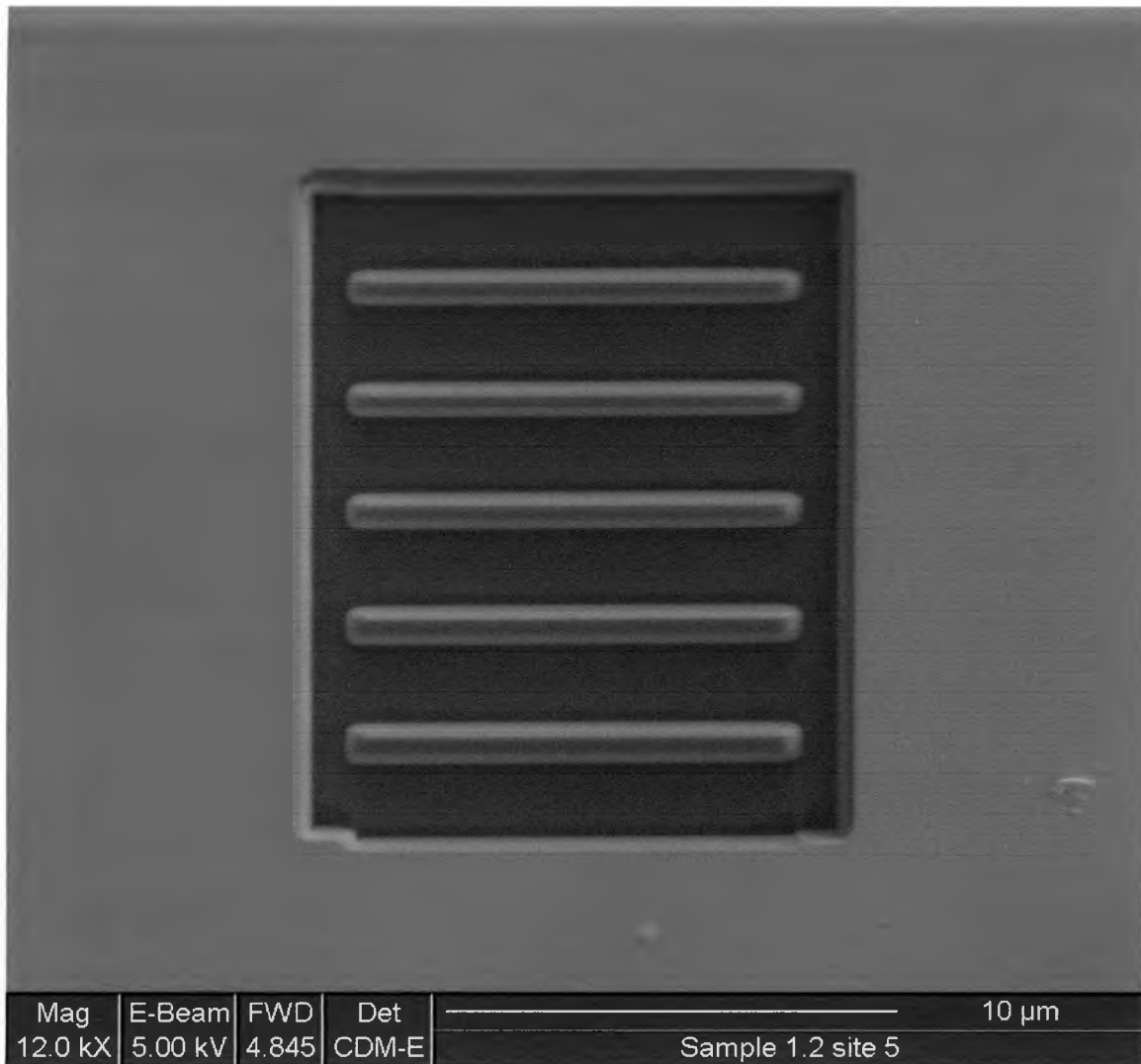


Figure 3-16: Serial mode with all regions being milled at the same time. 862pA beam current. minutes. The machined wires are much cleaner. This technique was used for all subsequent micromachining.

3.4.2 SAMPLE 3

Sample 3 was sample SWT 1.4 provided by Texas State. The films deposited on SWT 1.4 were 10Å of NiFe, 100Å Ta, 500Å NiFe and 100Å of Ta on a silicon substrate. The first run was an attempt to micromachine

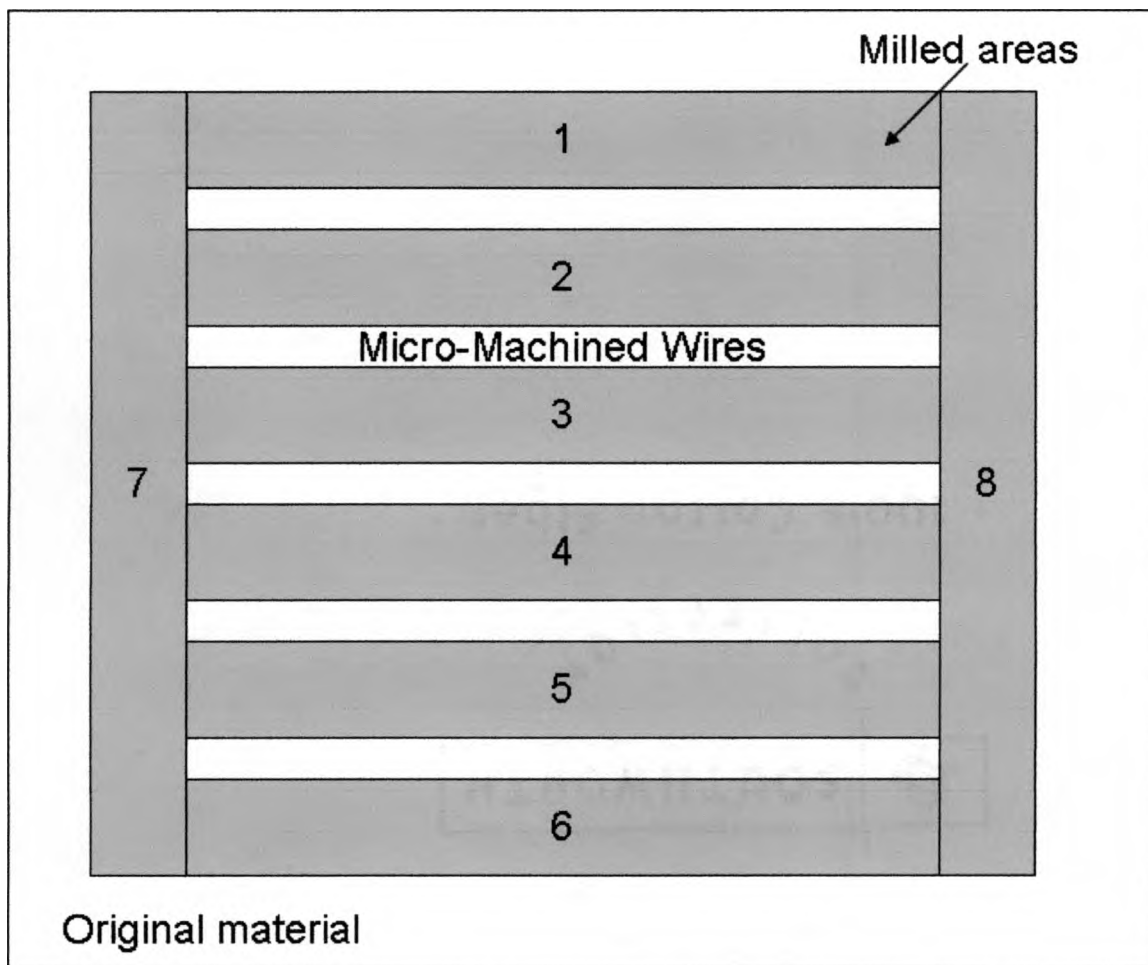


Figure 3-17: Mill pattern for first sample. Areas are numbered in order of the mill sequence. Mill patterns were $12 \times 2 \times 1 \mu\text{m}$. $1 \mu\text{s}$ dwell time, 50% overlap, 350pA beam current, $2.6 \mu\text{A}$ emission current. Sections 1-6 were milled in parallel followed by sections 7 and 8.

wires similar to the pattern in Figure 3-17. Using the learning from earlier work, zones 1 through 6 were milled at the same time. (Figure 3-18) This was followed by milling zones 7 and 8 to isolate the wires. (Figure 3-19) There were several problems with this method. To begin with each sequential cut was redepositing into a previously cleared area. This was caused in part by the selected pattern as well as discrepancies with the tool. For each of these cuts, 500pA was requested for the beam

current however problems with the tool caused the sample to get 900pA which aided the redeposition of material. A clean up mill was attempted to try and remove the redeposited material however this had undesirable effects on the machined wires. (Figure 3-20) This was further proof that for clean, micromachined structures, it is better to use the low beam current and mill all zones at the same time.

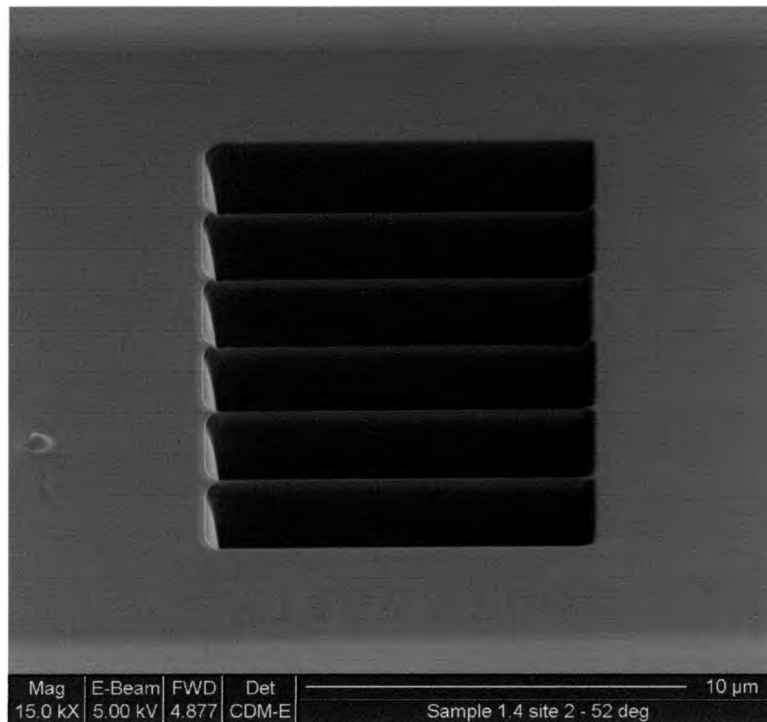


Figure 3-18: Initial parallel mill of six section to create the wires.

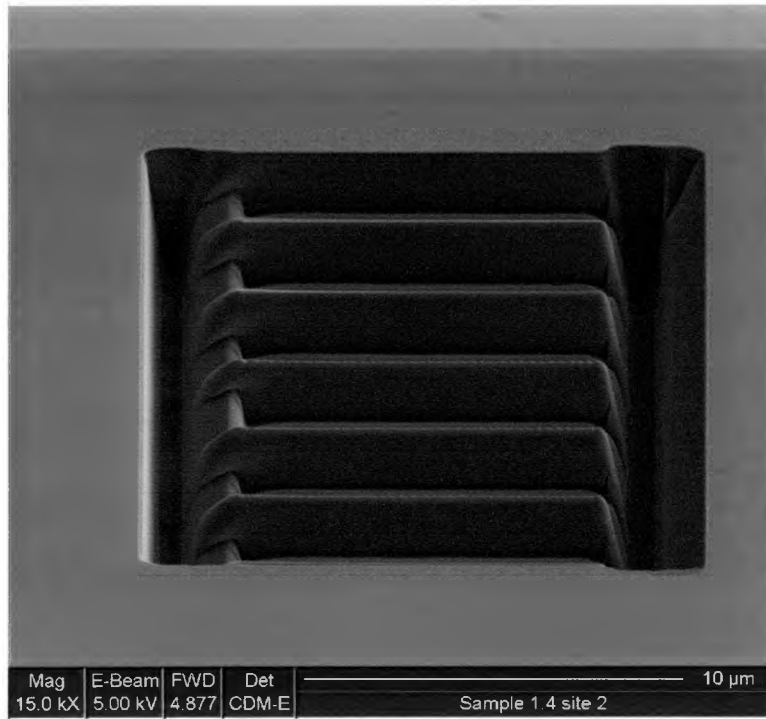


Figure 3-19: Isolation of the wires from the rest of the substrate.

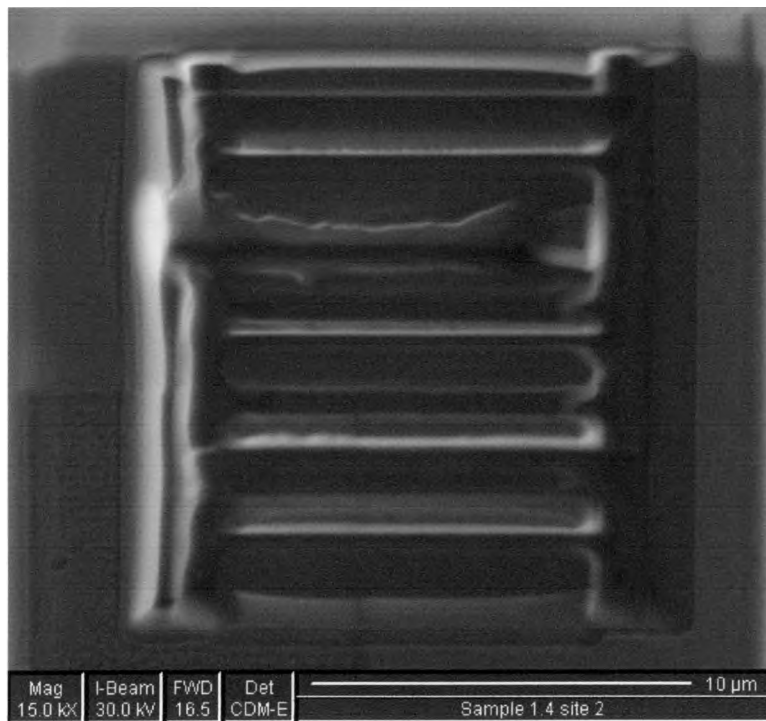


Figure 3-20: Attempts to remove the redeposited material ruined the machined wires.

3.4.3 Complex Shapes

Micromachining wires had a rocky beginning but lessons learned were easily translated to complex shapes. The most complicated part of complex shapes was selecting the correct beam current and adjusting the mill to leave the “slag” (redeposited material) in areas that would not interfere with the final desired shape. The first shape that was attempted was a circle

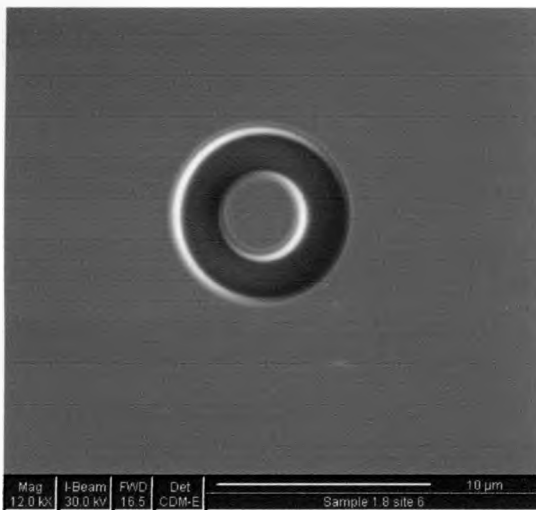


Figure 3-21: Ion beam image of micromachined circle.

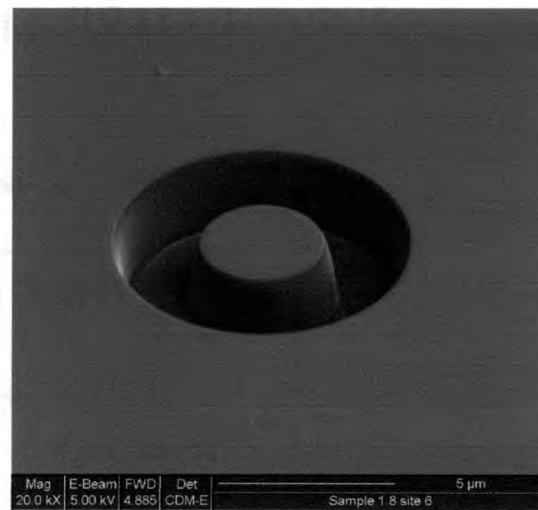


Figure 3-22: SEM image of same circle at 52° tilt.

Being able to successfully micromachine a circle was the first step to machining multiple cylinders in a pattern. This was accomplished using a repeated pattern of cylinders and rectangles that represented where the beam would mill. (Figure 3-23) Machining the cylinders highlighted an interesting side effect of milling through materials of any considerable depth. All cylinders in Figure 3-24 have a smaller radius at the top than they do at the bottom. This is from longer exposures to the ion beam.

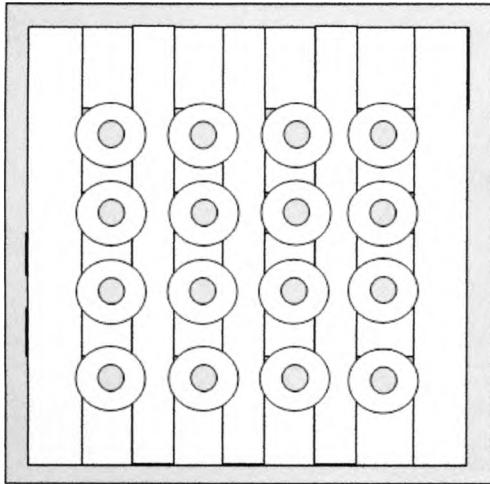


Figure 3-23: Mill Pattern for Cylinders

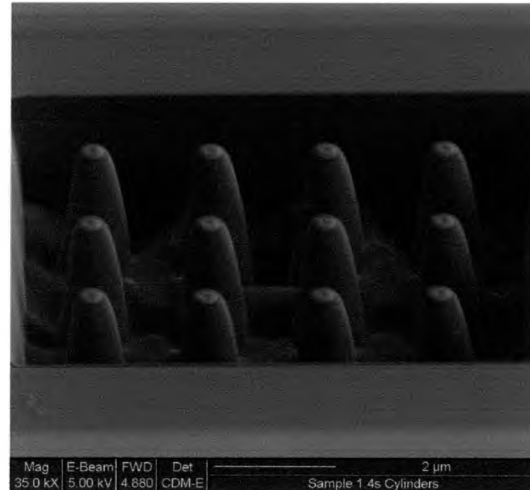


Figure 3-24: Micromachined cylinders.

Even though not directly in line with the beam incidental ion bombardment wears the tops away.

Milling hexagons turned out to be the most difficult to accomplish. This had a lot to do with the size of the hexagon required to survive the

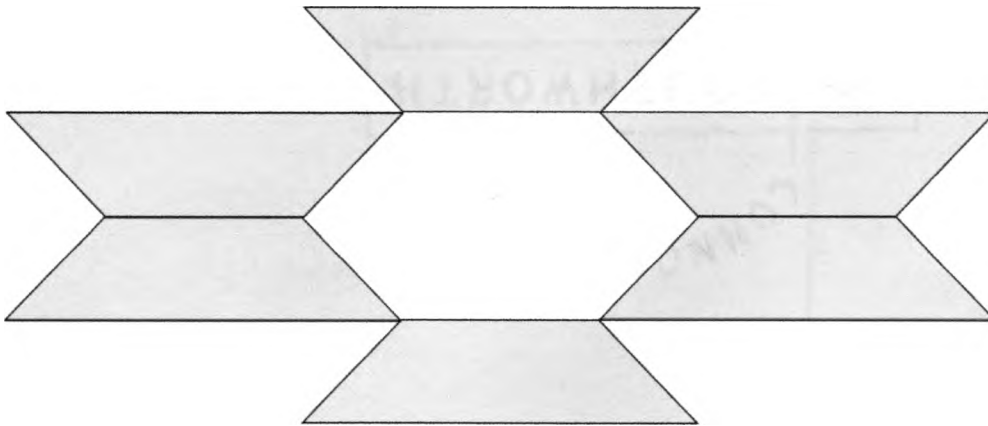


Figure 3-25: Mill pattern for milling hexagons.

milling. The pattern was created by using multiple parallelograms to create the shape of the hexagon. When smaller shapes were attempted the walls of the hexagon adjacent to the areas being milled would erode

away leaving a small stub rather than a hexagon. This was due to the beam path and the incidental damage impinging on the walls from multiple angles. Figure 3-26 shows the final results for machining

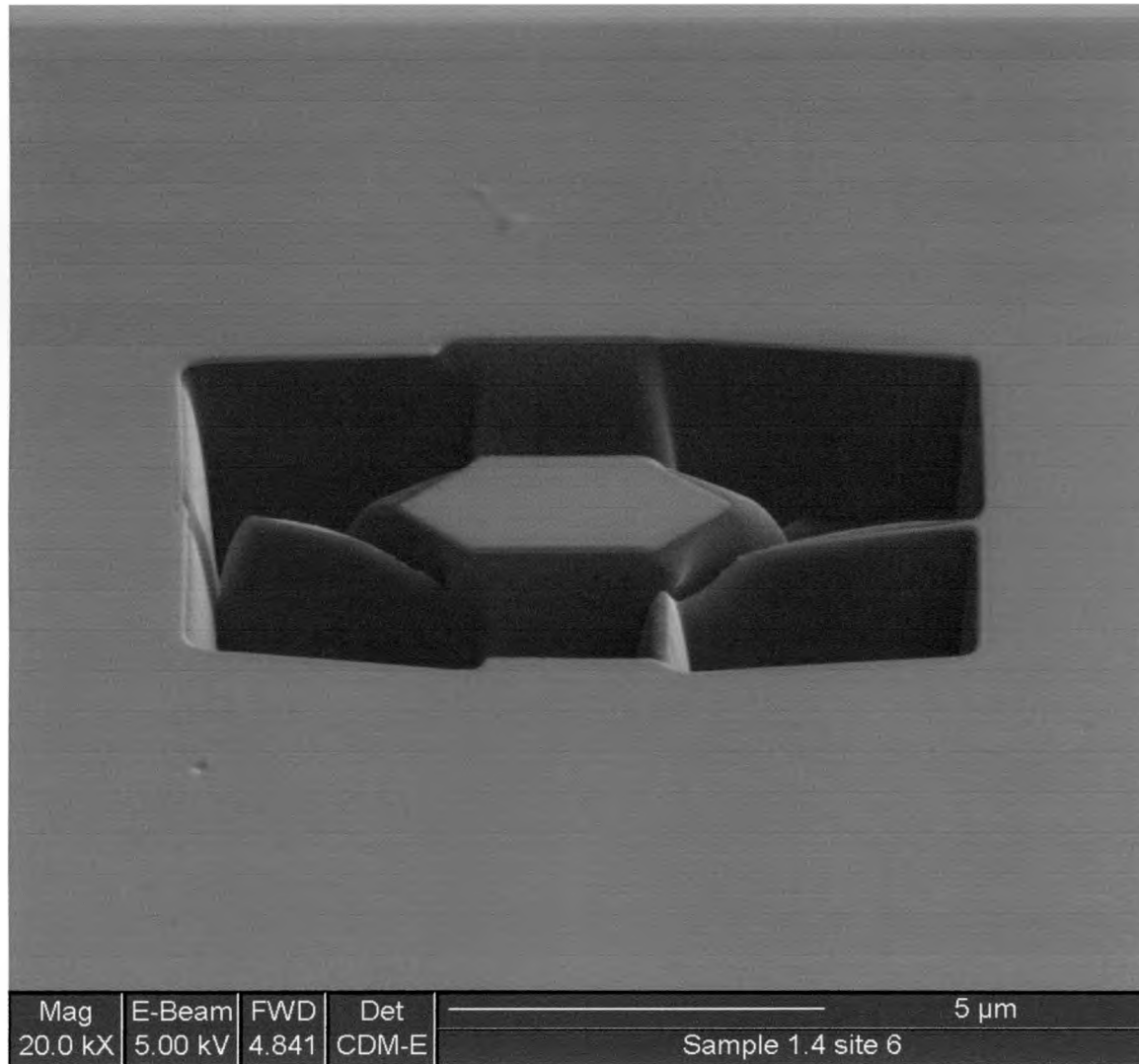


Figure 3-26: Micromachining hexagons turned out to be the most difficult shape to machine. hexagons. With additional tuning it may have been possible to machine the larger hexagons but since there was not a need for larger ones no further work was attempted.

Following these special shapes the focus returned to machining wires and more specifically serpentine wires and longer wires. The serpentine part was a modification of milling straight wires (Figure 3-27).

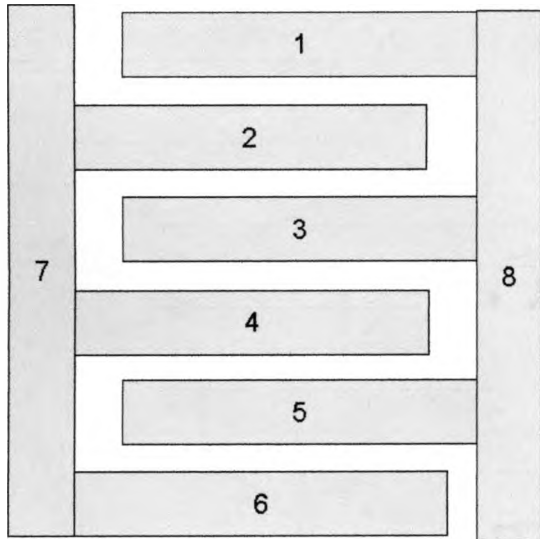


Figure 3-27: Mill pattern for serpentine structures. 800pA Beam Current.

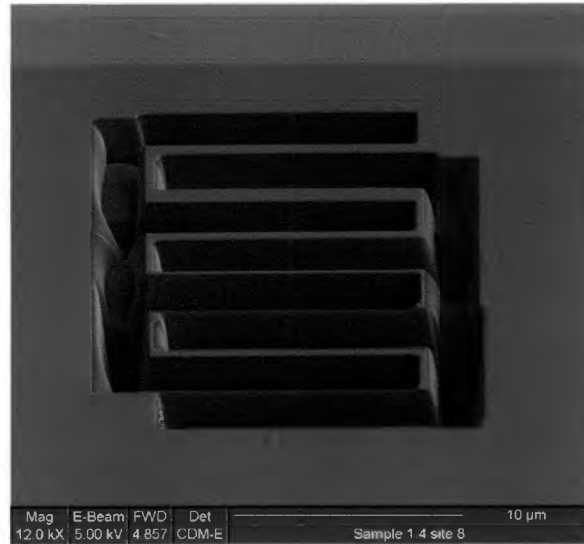


Figure 3-28: SEM image of micromachined serpentine.

The results were okay although at the turns there was some unexpected

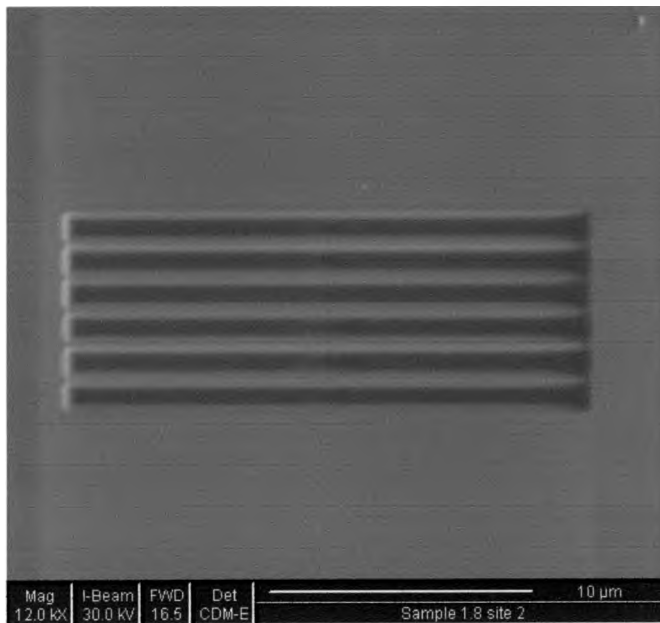


Figure 3-29: Micro wires twice as long as previously.

redeposition. (Figure 3-28) Included in the revisit to micromachining wires was machining wires twice as long as before. This was accomplished the same way as earlier wires.

Another sample, donated by Dr. Geerts, was used for milling grating patterns for various experiments to be performed at a later date.

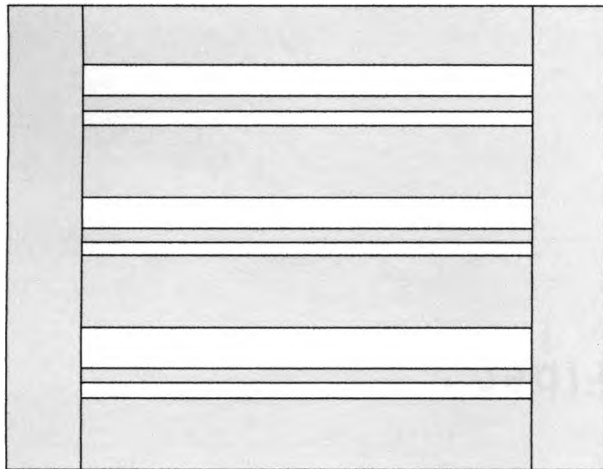


Figure 3-30: Grating pattern.

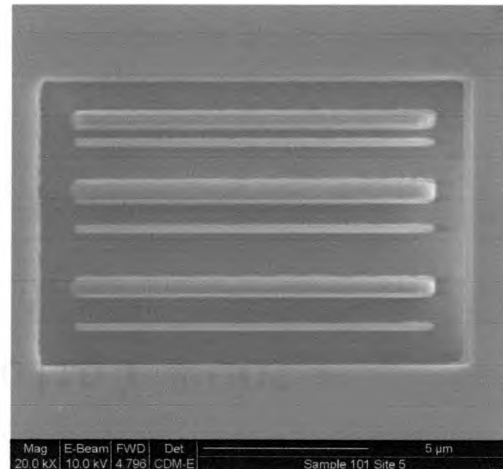


Figure 3-31: Milled grating.

Figure 30 shows the results of micromachining a grating structure. This mill was done in series with 872pA and was only 0.5 μ m's deep.

Each of these examples demonstrates the versatility of the tool. It is also evident that each type of material and each job require adequate understanding of the material properties and the correct setup to get the desired results.

CHAPTER 4

CONCLUSION

The focused ion beam is a versatile tool with a wide range of applications. The principal, systems, operation and techniques of the focused ion beam system were discussed in this thesis. The theories and applications of the FIB were investigated in the work performed throughout the course of this study. It was shown that a FIB can be used to remove material as well as deposit material, both of which have a wide range of uses.

The FIB is a simple and complex tool. Simply, it is the combination of an ion source, a column with focusing optics and a sample stage. More complicated it is method by which the ions are extracted from the source and focused with precise control onto the sample surface for either construction or destruction. It has been found that the most practical sources are liquid metal ion sources most commonly made up of gallium extruded onto a tungsten substrate. This source, when placed into an electric field, will generate a steady stream of ions that are accelerated and focused through the column. The column consists of a beam blanker, a blanking aperture and deflection plates. The beam blanker shifts the beam to and from the blanking

aperture turning the beam off and on. The deflection plates control the point at which the beam interfaces with the sample surface. Advanced computer controls make it possible to control this beam very precisely making precision milling possible.

In the field of semiconductor manufacturing the FIB can be used as a failure analysis tool for precision cross sections. In some cases this is performed inline preventing the need to scrap the whole wafer. It is also possible to rewire or change the circuitry of an integrated circuit using the milling and material deposition capabilities of the tool. The ion beam can be used to mill vias or lines and then filling them with a metal. It is also possible to deposit dielectrics to isolate features electrically. In this thesis the failure analysis capabilities of the FIB were demonstrated by isolating and milling down to an electrical failure making it possible to see the defective area. The FIB's deposition techniques were utilized to deposit an area of platinum on the circuit's surface to act as a hard mask for milling in a sensitive area. The hard mask protected features near the surface from the incidental damage of the ion beam leaving the area of interest intact.

The FIB is also a powerful tool for micromachining. The FIB's ability to micromachine various shapes into different materials was demonstrated. Wires were machined into various metal surfaces for additional experiments from Dr. Carlos Gutierrez. The micromachining capability of the FIB was demonstrated by milling out 10 μ m wires,

serpentine structures, cylinders and circles as well as an attempt at machining a hexagon.

It was found through the course of using the FIB for failure analysis and micromachining that different techniques should be employed depending on the application. In the area of failure analysis it was advantageous to do a quick parallel mill to remove the bulk material and follow up with a fine serial mill to expose the surface of the area of interest. This technique, however, was not beneficial in the area of micromachining structures. It was found that a slow serial mill of all of the individual zones in parallel was the most effective method. This prevented an assortment of artifacts from being left in and around the mill zone.

Each of these applications can be very useful in industry and save valuable manufacturing time when employed correctly. The failure analysis capabilities make it possible to look at product inline making it possible for changes to be made immediately rather than waiting until the product has reached the end of the line to find out where mistakes were made. The FIB provides an effective method for rewiring and testing prototype circuits. It is also very effective in micromachining micro-devices for MEMS applications or other test vehicles. Overall, this tool is becoming a very important tool in many different industries.

BIBLIOGRAPHY

- ¹ Beck, Friedrich. *Integrated Circuit Failure Analysis: A Guide to Preparation Techniques*. John Wiley & Sons, 1998.
- ² Wagner, Lawrence C., Ed. *Failure Analysis of Integrated Circuits: Tools and Techniques*. Kluwer Academic Publishers, 1999.
- ³ Melngailis, John. "Focused Ion Beam Technology and Applications." In *Journal of Vacuum Science and Technology*, B5(2). Mar/Apr 1987.
- ⁴ Helbert, John N. Ed. *Handbook of VLSI Microlithography: Principles, Tools, Technology and Applications*. Noyes Data Corporation/Noyes Publications, 2001.
- ⁵ Krueger, Robert. "Dual-Column (FIB-SEM) Wafer Applications." In *Micron* 30 221-226, 1999.
- ⁶ Tao, Tao, William Wilkinson, and John Melngailis. "Focused Ion Beam Induced Deposition of Platinum for Repair Processes." In *Journal of Vacuum Science and Technology*, B9(1). Jan/Feb 1991.
- ⁷ Ishitani, Tohru, Yoshimi Kawanami. "Coarse Guidelines in Designing Focused Ion Beam Optics." In *Journal of Vacuum Science and Technology*, B13(2). Mar/Apr 1995.
- ⁸ *Introduction: Focused Ion Beam Systems*. Filmetrics, Inc., San Diego: <http://www.filmetrics.com>.
- ⁹ Kirch, S.J., D.J. Tomasi. "Advanced Micromachining Techniques for Failure Analysis." 17th ISTFA, 1991.
- ¹⁰ Shaver, D. C., B.W. Ward. "Semiconductor Applications of Focused Ion Beam Micromachining." In *Solid State Technology*, December 1985.
- ¹¹ Orloff, John, Mark Utlaut, and Lynwood Swanson. *High Resolution Focused Ion Beams: FIB and Its Applications*. Kluwer Academic/Plenum Publishers, 2003.

- ¹² Caney-Peterson, Susan, Judy Lane Green, Ellen Adams, Kristen Geiger, Susan Gilpin, Erin Sunahara, Wyn Bowler. *xP DualBeam Workstation Reference Guide*. FEI Company, 1999.
- ¹³ Caney-Peterson, Susan, Judy Lane Green, Ellen Adams, Kristen Geiger, Susan Gilpin, Erin Sunahara, Wyn Bowler. *xP DualBeam Workstation User's Guide*. FEI Company, 1999.
- ¹⁴ Nikawa, K. "Applications of Focused Ion Beam Technique to Failure Analysis of Very Large Scale Integrations: A Review." In *Journal of Vacuum Science and Technology*, B9(5). Sep/Oct 1991.

VITA

Nelson W. White II was born May 28, 1971 in Austin, Texas, to Nelson and Gail White. In the summer of 1989 he enrolled at Texas State University – San Marcos. While working many part time and full time jobs to pay for school he continued his studies and graduated in December of 1997 with a Bachelor of Science in Physics. He worked for Electrosorce Battery Company in San Marcos following graduation as a research scientist and shortly thereafter, due to the declining health of the company, he joined VLSI Technologies in San Antonio where he began his career in the semiconductor industry. In the fall of 1998 he enrolled in the graduate college of Texas State University while excelling as a full-time employee at Philips Semiconductors, formerly VLSI Technologies, as a CMP Process Engineer where he had two patents issued (Pat. No. 6,537,141 - Non-slip polisher head backing film; Pat. No. 6,409,579 – Method and apparatus for condition a polish pad at the point of polish and for dispensing slurry at the point of polish) in his name and several pending. In addition to the two patents he coauthored “Failure rate and yield-limiting tungsten plug corrosion diagnosis using characterization test vehicles”, along with several of his colleagues, published in Advanced Semiconductor Manufacturing 2002

IEEE/SEMI Conference and Workshop. While finishing his course work on pace with the other full time students his thesis was delayed during the illness and death of his father as well as his new responsibilities at work following his promotion to CMP Engineering Manager at Philips Semiconductors in San Antonio. Through the support of family, friends and Dr. Carlos Gutierrez, he continued slow progress on his thesis until an unfortunate downturn in the semiconductor industry forced the closure of Philips Semiconductors in San Antonio, freeing him to continue his research. During this time he also earned his private pilots license. Shortly after the closure of Philips Semiconductors he was hired as a Senior Research and Development CMP Engineer with Micron Technologies in Boise, Idaho. During this time he continued work on his thesis completing it in January 2005.

Permanent Address: P.O. Box 640
Blanco, Texas 78606

This thesis was typed by Nelson W. White